# FAST AMPLITUDE AND DELAY MEASUREMENT FOR CHARACTERIZATION OF OPTICAL DEVICES

A Thesis

by

MICHAEL THOMAS THOMPSON

Submitted to the Office of Graduate Studies of
Texas A&M University
in partial fulfillment of the requirements for the degree of

MASTER OF SCIENCE

August 2006

Major Subject: Electrical Engineering

# FAST AMPLITUDE AND DELAY MEASUREMENT FOR CHARACTERIZATION OF OPTICAL DEVICES

A Thesis

by

MICHAEL THOMAS THOMPSON

Submitted to the Office of Graduate Studies of
Texas A&M University
in partial fulfillment of the requirements for the degree of

MASTER OF SCIENCE

Approved by:

| | |
|---|---|
| Chair of Committee, | Christi Madsen |
| Committee Members, | Steven Wright |
| | Alvin Yeh |
| | Chin Su |
| Head of Department, | Costas Georghiades |

August 2006

Major Subject: Electrical Engineering

## ABSTRACT

Fast Amplitude and Delay Measurement for Characterization of Optical Devices. (August 2006)

Michael Thomas Thompson, B.S., Louisiana Tech University

Chair of Advisory Committee: Dr. Christi Madsen

A fast measurement technique based on the modulation phase-shift technique is developed to measure the wavelength-dependent magnitude and phase responses of optical devices. The measured phase response is in the form of group delay, which is used to determine the chromatic dispersion in the device under test by taking the derivative of the group delay with respect to optical wavelength. The measurement setup allows both step-tunable and sweeping laser sources. A modulation frequency of up to 2.7 GHz is accommodated. An alternate method for the phase measurement that overcomes non-linearities in the measurement setup is also presented. The speed of the measurement setup is limited by the sweeping speed of the laser source, which for the Agilent 81682A is 40 nm/sec. The magnitude accuracy is determined by taking a comparison to the commercially available Micron Finisar measurement system, where an error of 0.125 dB is noted. The phase accuracy of the measurement setup is tested by taking the Hilbert transform of the measured magnitude response of an Acetylene gas cell and comparing it to the integral of the measured group delay. The average deviation between the two methods is 0.1 radians. An Acetylene gas cell, fiber Bragg grating, and chirped Bragg grating are tested with the measurement setup and the Agilent 81682A laser source at 40 nm/sec and the measurement plots are presented.

The characterization of the setup leads to the conclusion that the measurement setup developed in this paper is fast and accurate. The speed of the technique is on the order of microseconds for a single measurement and excels beyond the speed of the standard modulation phase-shift technique, which includes measurement times on the order of minutes. The accuracy of the technique is within 0.125 dB for magnitude measurements and 0.1 radians for phase measurements when compared to commercially available measurement systems.

To my parents Roger and Connie, and my siblings Pete and Jenny

## ACKNOWLEDGMENTS

I would like to thank my committee chair, Dr. Madsen, and my committee members, Dr. Wright, Dr. Yeh, and Dr. Su, for their guidance and support throughout the course of this research. I would also like the thank Dr. Madsen for access to her laboratory and equipment.

Thanks also to my friends and colleagues and the department faculty and staff for making my time at Texas A&M University a great experience. I also want to thank Donald Adams, Mehmet Solmaz, Hui Zhu, and William Rivera for their help in this research project.

Finally, I would like to thank my parents, brother, and sister for their encouragement and support.

# NOMENCLATURE

| | |
|---|---|
| DPS | Differential Phase-Shift |
| FM | Frequency Modulation |
| MPS | Modulation Phase-Shift |
| PEC | Phase-Error Compensation |

# TABLE OF CONTENTS

# LIST OF FIGURES

FIGURE Page

# LIST OF TABLES

# INTRODUCTION

Dispersion plays a vital role in the performance of today's fiber optic systems. The information carrying capacity of optical fibers and devices is limited by dispersion, which causes pulse broadening. As demand for bandwidth increases, optical pulses are placed closer together, so that the amount a pulse can spread before overlapping other adjacent pulses greatly decreases. Chromatic dispersion is a major concern when trying to maximize the efficiency of an optical communication system. As multi-stage filters become more commonplace, the need for faster methods to characterize these devices is present. In order to characterize these devices completely, the magnitude and phase responses are required. There are several techniques presently that will measure the phase response of optical devices in the form of group delay. The ability to also measure the magnitude response of a device increases the complexity of the measurement setup. Polarization dependence, temperature drift, drifts in waveguide coupling, and vibrations can cause errors in the magnitude and phase measurements. Therefore, higher speed is crucial in improving accuracy to alleviate these error sources as well as increasing the economic viability of the measurement setup.

Two popular methods to determine the phase response of an optical device include the modulation phase-shift technique and the interferometric technique. The modulation phase-shift technique measures group delay, determined by the phase shift

---

This thesis follows the style of *Journal of Lightwave Technology*.

between a reference signal and a signal that travels through a device under test, each of which originates from the same source. The interferometric technique measures the optical phase with regard to optical frequency directly. The interferometric technique by its very nature is much more sensitive to temperature, vibrations, and polarization than the modulation phase-shift technique. The measurement technique developed in this research work is based on the modulation phase-shift technique, but is much faster. Phase measurement time is such that a sweep of the modulation frequency can be implemented along with a sweep of the laser wavelength. The measurement time for a single measurement at a specific wavelength is on the order of microseconds with this new method. For measuring over a wavelength range, the measurement speed is only limited by the sweep speed of the laser source, which in our case is 40 nm/sec. The absolute magnitude measurement accuracy was found to be within 0.125 dB when compared to the commercially available Micron Finisar measurement system. The absolute phase accuracy was determined by integrating the measured group delay to obtain the optical phase reponse and then comparing it to the ideal optical phase, obtained by taking the Hilbert Transform of the measured magnitude data. The absolute phase accuracy was found to match the ideal optical phase with an average deviation of 0.1 radians.

# CHROMATIC DISPERSION

## Overview

There are four different types of dispersion: intermodal, polarization-mode, material, and waveguide. Intermodal dispersion occurs when an optical signal splits into multiple modes that travel at different velocities, affecting multimode devices. Polarization-mode dispersion is due to stresses between the cladding and guiding core materials in dielectric waveguides. These stresses cause refractive index differences to develop between different polarizations. Material dispersion occurs due to the dependence of the refractive index on wavelength. Waveguide dispersion is caused by the dependence of the propagation constant, $\beta$, on wavelength. Chromatic dispersion, the most predominant form of dispersion in single-mode fibers, is the term given to the combined effect of material dispersion and waveguide dispersion. Chromatic dispersion is related to the group delay of an optical device by $D = d\tau_g / d\lambda$, where D is the chromatic dispersion, $\tau_g$ is the group delay, and $\lambda$ is the wavelength. The group delay of an optical device is related to the optical phase by $\tau_g = - d\Phi / d\Omega$, where $\tau_g$ is the group delay, $\Phi$ is the optical phase, and $\Omega$ is the optical radian frequency.

Material dispersion in a waveguide develops from the dependence of the refractive index on wavelength. A wavelength-dependent dielectric constant occurs when the electric field of light interacts with a dielectric material by displacing charges from their equilibrium positions. This phenomenon affects the velocity at which light travels through a material in relation to frequency. Therefore, the refractive index (ratio

of speed of light in vacuum to speed of light in a medium) is also frequency-dependent and can be approximated by the Sellmeir equiation:

$$n^2 - A_o \equiv \sum_{n=1}^{N} \frac{A_n \lambda^2}{\lambda^2 - \lambda_n^{\,2}}$$

For fused silica, $A_o = 1$, $A_1 = 0.6961663$, $A_2 = 0.4079426$, $A_3 = 0.8974794$, $\lambda_1 = 0.0684043$ μm, $\lambda_2 = 0.1162414$ μm, and $\lambda_3 = 9.896161$ μm.

When an optical pulse, consisting of components with different wavelengths, travels through a medium in which the refractive index is wavelength dependent, the wavelength components travel at different group velocities. This effect causes an optical pulse to spread. The equation for material dispersion in time (seconds) is

$$\Delta\tau \equiv -L \frac{\lambda}{C} \frac{d^2 n}{d\lambda^2} \Delta\lambda$$

where $\Delta\tau$ = dispersion in time, L = travel distance, $\lambda$ = wavelength, C = speed of light, and n = refractive index. The material dispersion coefficient is

$$D \equiv -\frac{\lambda}{C} \frac{d^2 n}{d\lambda^2}$$

with typical units of ps/(km-nm). The dispersion coefficient is a commonly used parameter to describe the dispersion for a pulse of 1 nm in spectral width, traveling a 1 km distance.

Waveguide dispersion occurs when the group velocities of modes are wavelength dependent due to the dependence of the propagation constant, β, on wavelength. This type of dispersion is typically the smallest among the different types. However, it is an important contributor to dispersion in singlemode waveguides when

the material dispersion is minimal. The equation of waveguide dispersion in time (seconds) is

$$\Delta\tau \equiv \frac{L}{C}\frac{d^2\beta}{dk^2}\Delta k$$

where $\Delta\tau$ = dispersion in time, L = travel distance, $k = 2\pi / \lambda$, C = speed of light, and $\beta$ = propagation constant. The waveguide dispersion coefficient (in ps/(km-nm)) is

$$D \equiv \frac{1}{C}\frac{d^2\beta}{dk^2}$$

The effects of both material dispersion and waveguide dispersion are commonly referred to as chromatic dispersion. Diagnosing the chromatic dispersion in an optical component is crucial, so that proper compensation can be implemented in the fiber optic network in order to maximize communication efficiency [1]. Of course, dispersion in optical filters is caused from the poles and zeros that arise from interference in the filters.

**Measurement Techniques for Chromatic Dispersion**

Today's higher bitrate applications require accurate methods of measuring dispersion for integrated optic devices. In order to fully characterize such devices, fast, accurate magnitude and phase measurements of the device with respect to wavelength are required. Not only is there a demand for fast measurement techniques to overcome measurement inaccuracies due to waveguide coupling, polarization dependence, or temperature drift, but also for economic efficiency. Faster measurement speed is a

helpful tool in characterizing more complex, integrated, and tunable optical circuits seen in industry today.

There are currently five predominant methods to determine chromatic dispersion in optical devices: the modulation phase-shift method, differential phase-shift method, time-of-flight method, interferometric method, and the Hilbert transform. The modulation phase-shift method is the most popular technique used today.

The modulation phase-shift (MPS) method was first mentioned in [2], where actual development of the technique is reported in [3,4], in which B. Costa et al recorded accuracies of 2 picoseconds in relative group delay and of ±1 ps/nm-km in chromatic dispersion measurements. More recently, T. Dennis and P.A. Williams recorded accuracies of ±0.46 ps in group delay [5]. The technique consists of sinusoidally modulating a light source, in which one of two signal paths acts as a reference channel, while the other light path traverses through a device under test [6]. Both signal paths are then compared and a measurable phase shift is detected between them, resulting in a measured group delay (time delay) as a function of wavelength, caused by the device under test. The phase shift detected is equal to the modulation frequency times the group delay between the two signal paths. Due to the nature of the setup, multiple period shifts of delay can give deceiving results. Therefore, it is important that caution be taken so that this aliasing effect is avoided to improve accuracy. The measured group delay, retrieved from the relationship to the measured phase shift and modulation frequency, is then used to determine the chromatic

dispersion in the device under test. The modulation frequency plays a direct role in the resolution of the group delay measurement.

The differential phase-shift (DPS) method is based upon the modulation phase-shift method, however, the wavelength of the laser source is dithered around a central wavelength [7,8,9,10]. Building on the MPS method, the DPS method introduces a wavelength selector in the DUT path to control the wavelength dither. The DPS method directly determines the value of chromatic dispersion at a selected wavelength by averaging the detected dispersion over a dithered wavelength interval. Since the DPS method averages dispersion, it is faster than the MPS method, but also has low resolution and less accuracy because of the same process [8].

The time-of-flight method, also known as the 'pulsed light method,' requires extremely accurate measurement of pulse arrival times [11,12]. The method requires the use of Raman systems for the generation of pulses, which add jitter and optical triggering instabilities to the setup. Overall, the time-of-flight method is cumbersome, expensive, and relatively inaccurate [3].

The interferometric method involves using a basic Mach-Zehnder interferometer setup where one leg of the interferometer is a reference path and the other leg is a device under test [13]. This method measures optical phase directly through interference techniques, which allows high resolution and accuracy of 1 picosecond in group delay. Since there is not an extra calculation step to determine the optical phase performance of the device under test like that seen in the MPS and DPS methods, the accuracy of the interferometric method is slightly greater [14]. However,

due to the interferometer setup, many other sources of error like fiber stabilization play a huge role in accuracy. The interferometric method is limited, due to the fact that the reference path needs to be approximately the same length as the device under test optical path.

If an optical filter fulfills the 'minimum phase condition,' then the amplitude and phase responses of the filter are related by the Hilbert transform [7,1]. The criterion for minimum phase is if all of the zeros of the filter are inside the unit circle. Filters with all-pole responses are considered minimum phase. The phase response and dispersion of such a filter can be directly determined from the amplitude response [1]. Unfortunately, many optical devices do not meet this criterion.

# MEASUREMENT SETUP

## Overview

The measurement technique discussed in this thesis is based on the modulation phase-shift technique. The typical setup for the MPS technique consists of a sinusoidal wave generator with a typical frequency range of approximately 30 MHz to 3 GHz, tunable laser source, optical amplitude modulator, high speed detector, and a phase detector. A general block diagram can be found in Figure 1.

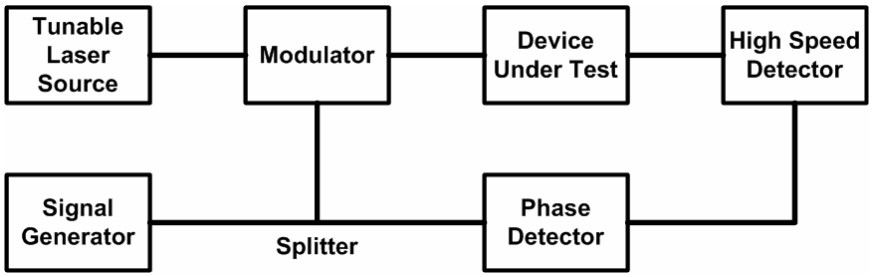


Fig. 1. Modulation Phase-Shift Technique Block Diagram

The general idea behind the technique is to amplitude modulate the light traveling through an optical device under test, retrieve the signal out of the device under test, and compare it to the original signal that drove the amplitude modulation. In so going, the delay versus wavelength that the device under test induces upon the test path signal can be measured in the form of phase shifts between the two measured signals. For example, the sinusoidally modulated optical modulator causes the light traveling through the device under test to have a detected photo current amplitude, i(t), to be

directly proportional to $\cos(\omega_m t - \varphi)$, where $\varphi$ is the wavelength dependent phase shift that occurs from the dispersion of the device under test. As the signal travels through the device under test, its phase changes according to $\varphi(\lambda) = 2\pi f_m \tau(\lambda)$, where $\varphi(\lambda)$ is the wavelength dependent phase, $f_m$ is the modulation frequency, and $\tau(\lambda)$ is the wavelength dependent group delay. Unlike the interferometric technique, the MPS technique is insensitive to optical phase, such that the wavelength dependent delay of the optical path, $\tau(\lambda)$, is measured.

The MPS technique allows the chromatic dispersion of a device to be determined by measuring the group delay versus wavelength of the test device and taking the derivative to find the chromatic dispersion. The modulation frequency, $f_m$, affects the resolution of the measurement simply from the equation $\tau(\lambda) = \varphi(\lambda) / 2\pi f_m$. A higher $f_m$ allows a smaller group delay resolution. However, care must be taken in order to avoid a measurement wrap around when the measured signal phase shift, $\varphi(\lambda)$, encounters multiples of $2\pi$. Therefore, it is customary to determine the maximum measurable group delay for a particular modulation frequency (without encountering the $2\pi$ wrap around error) which is simply $\tau(\lambda) = 1 / f_m$.

Another object of importance is the selection of the phase detector. The accuracy of the phase detector directly determines the performance of the technique. The most popular phase detector used currently is a lock-in amplifier, with an accuracy of approximately 0.1 degrees. However, lock-in amplifiers of this caliber are costly and slow. If a lock-in amplifier is used, a heterodyne technique should be employed. For example, a 100 MHz sinusoidal signal could drive the optical modulator and then

be mixed with a 100.01 MHz signal to form the reference channel of the lock-in amplifier. The high speed optical detector signal is then mixed with the 100.01 MHz and used as the test signal for the lock-in amplifier. Then, the 10 kHz signals with the same phase characteristics as the reference and test channels can be compared. Keeping the accuracy of the phase detector in mind, the modulation frequency, $f_m$, has a close connection to the overall accuracy. For example, the overall accuracy with a phase detector accuracy of 0.1 degrees (for $\varphi(\lambda)$) is directly determined by the selection of the modulation frequency, $f_m$. If the phase detector accuracy is 0.1 degrees, then the accuracy of the measurement from the phase detector's standpoint is simple 0.1 degrees multiplied by the group delay resolution determined by the modulation frequency. A reference table comparing different modulation frequencies and group delay measurements can be found in Table 1.

Table 1. Group Delay Measurement Resolution

| Modulation Frequency | Group Delay Resolution (ps) | Group Delay Max (ps) |
|---|---|---|
| 100 MHz | 27.78 | 10000 |
| 500 MHz | 5.56 | 2000 |
| 1 GHz | 2.78 | 1000 |
| 1.5 GHz | 1.85 | 667 |
| 2 GHz | 1.39 | 500 |
| 2.5 GHz | 1.11 | 400 |
| 3 GHz | 0.93 | 333 |

## Modified Phase-shift Technique

### *Setup*

The motivation behind this research project included a much faster and less expensive way to measure chromatic dispersion in optical devices. As discussed before, lock-in amplifiers offer accuracy at the expense of cost and time, so a cheap alternative phase detector would be necessary. The objective of the project included a measurement setup composed of typical optical laboratory components.

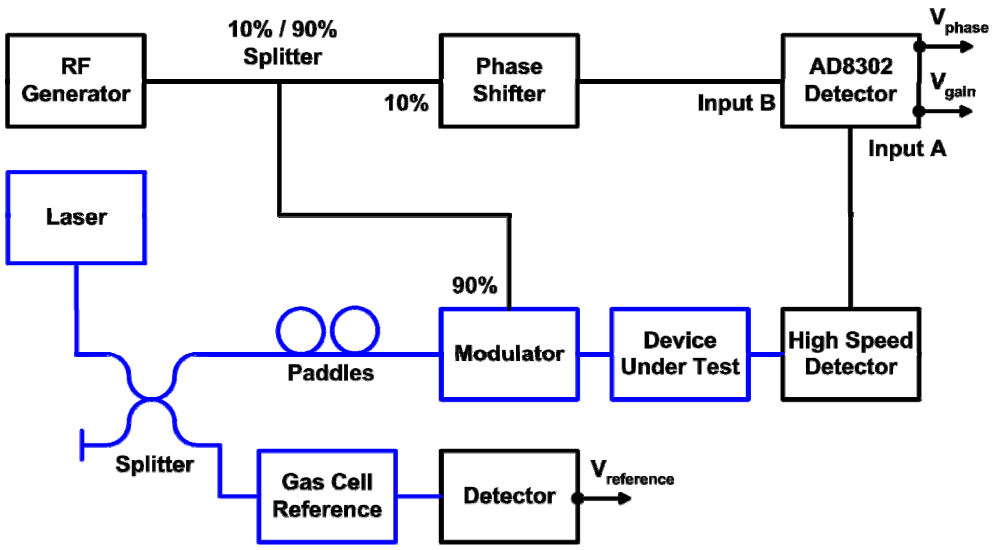


Figure 2. Modified Phase-Shift Technique Setup

A block diagram of the new measurement setup focused on in this research paper is shown in Figure 2. In Figure 2, the optical path includes the laser, splitter, paddles, gas cell reference, modulator, and device under test while the electrical path includes the RF generator, 10% / 90% splitter, phase shifter, detector, high speed

detector, and the AD8302 detector. The new measurement setup is of course based on the modulation phase-shift technique as previously stated. One important difference is that the new setup incorporates a logarithmic amplifier phase detection scheme in the form of the Analog Devices 8302 magnitude/phase detector. With the use of this chip, a single frequency sinusoidal signal is generated without the need of the heterodyne technique required with a lock-in amplifier. A RF wave generator was selected for this signal generation. Other components in the setup include a 10%-90% RF splitter, tunable laser source, optical amplitude modulator with polarization paddles, manual RF phase shifter, and a high speed optical detector. An Acetylene gas cell and optical detector is integrated through a splitter in order to provide wavelength referencing for the laser supply.

The measurement setup operates by generating a sinusoidal signal from the RF generator which is split in two paths, where one path (10% RF signal) is used as a reference channel and the second path (90% RF signal) is used to drive the optical modulator. The reference RF signal passes through a RF phase shifter, which can be used for calibration, and then acts as the reference input (Input B) for the AD 8302 detector chip. The AD 8302 chip measures the magnitude and phase between two input channels and outputs corresponding voltages for the magnitude ratio ($V_{gain}$) and for the phase difference ($V_{phase}$). A tunable laser is used as the optical source in which the output of the laser is split in two paths, where one path travels through polarization paddles and on to the optical modulator and the second path travels to the wavelength referencing setup. The optical modulator is polarization dependent and therefore

requires a polarization transformer, implemented using rotating fiber in the form of paddles to align the input polarization to one of the principle axes of the modulator. The process of finding the correct polarization for the modulator is simple. First, DC bias is applied to the bias input of the modulator in order to find the minimum output optical power. Next, the polarization paddles are adjusted so that the minimum in optical power from the output of the modulator is more precisely located. Following this, the DC bias is decreased until a maximum in optical power from the output of the modulator is found. Finally, the DC bias is increased until the output optical power of the modulator is decreased by 3 dB from the maximum optical power output. The output of the optical modulator travels through the device under test, where it encounters a wavelength-dependent delay. After the device under test, the optical path continues to the high speed optical detector and then to the AD 8302 (Input A). An advantage of using the AD 8302 for phase detection is that a magnitude measurement is available so that both the magnitude and phase characterization of a device under test can be measured.

The hardware used in the measurement setup is commonly found in many optical laboratories. Laser sources tested with this setup include the HP 8168 step-tunable laser source and the Agilent 81682A sweeping laser source. Both types of lasers can be used with the setup; however the sweeping laser offers a much greater advantage in speed (40 nm/sec). A Wiltron 6637A-40 RF sweep generator and a HP 8350A RF sweep generator were tested in the setup. The high speed optical detector is an HP 83410C. The wavelength referencing detector consists of an InGaAs photo

detector and transimpedance op-amp circuit. The optical modulator is a Corning OTI SD-10-A. The splitters and polarization paddles are typical generic components. A computer with LabView software is used to communicate with the hardware in the setup and also record and process the measurement data. A National Instruments PCI 6115 data acquisition board was chosen for the data capturing. Specifications on all of these components can be found in Appendix A.

The Analog Devices 8302 chip is classified as a gain and phase detector. The chip uses demodulating logarithmic amplifiers to detect a gain difference (in dB) between two input channels. Phase detection is available by an onboard multiplier type phase detector. The AD 8302 has a gain measurement range from -30 dB to 30 dB with a measurement sensitivity of 30 mV/dB. The measurement range for phase detection is -180 degrees to 180 degrees with a sensitivity of 10mV/degree. In the measurement setup developed in this research work, the AD 8302 was put in measurement mode, where -90 degrees and 90 degrees are centered at 0.9 Volts. The AD 8302 allows other modes where the gain and phase curve slopes and center points can be altered by adding external components. Once a gain and phase measurement is taken between the two input channels, the AD 8302 changes output voltages $V_{gain}$ and $V_{phase}$ accordingly. The equations that determine these output voltages are as follows:

$$V_{gain} = 30 \text{ mV/dB} * (\text{Power}_A - \text{Power}_B) + 900 \text{ mV}$$

$$V_{phase} = -10 \text{ mV/degree} * (|\varphi_A - \varphi_B| - 90^{\circ}) + 900 \text{ mV}$$

where $\text{Power}_A$ and $\text{Power}_B$ are in dB, $\varphi_A$ and $\varphi_B$ are in RF degrees, and $V_{gain}$ and $V_{phase}$ are in Volts.

In conclusion, the measurement setup measures the wavelength dependent group delay in the device under test. The typical MPS equation becomes

$$\varphi(\lambda) = 2\pi f_m [\tau_{dut}(\lambda) - \tau_{setup}(\lambda)],$$

where $\varphi(\lambda)$ is the wavelength dependent RF phase, $f_m$ is the modulation frequency, $\tau_{dut}(\lambda)$ is the wavelength dependent group delay of the device under test, and $\tau_{setup}(\lambda)$ is the relative group delay between the optical path and the reference path of the measurement setup without a device under test.

### *Methods of Operation*

*Simple Method*

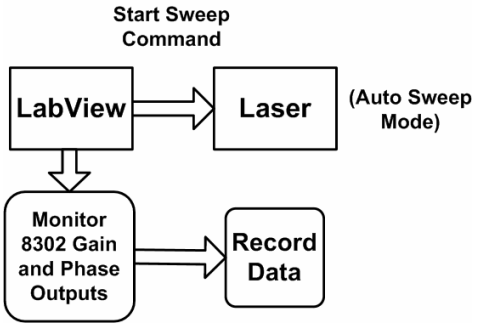


Figure 3. Measurement Setup Simple Method

The simple method, as seen above in Figure 3, consists of recording the output voltages ($V_{gain}$ and $V_{phase}$) as the laser source is stepped or swept through a particular wavelength range. Single point measurements are also available for a particular wavelength of interest. This method is simple; however it suffers from phase

measurement inaccuracies that arise from the phase detection scheme implemented in the AD 8302 chip. For example, the ideal $V_{phase}$ output of the AD 8302 would be a triangle waveform for a phase range of -180 degrees to 180 degrees, where the peak (1.8 Volts) occurs at the midline of 0 degrees. This ideal output can be found in Figure 4a. Realistically, the AD 8302 has non-linearities associated with the logarithmic amplifier phase detection scheme. The typical $V_{phase}$ output has error regions that give a 'rounding' effect on the ideal waveform. This effect can be seen in Figure 4b, taken from the AD 8302 data sheet for a 1.9 GHz frequency. As seen from Figure 4b, an accurate phase measurement can only be obtained in the regions of -120 degrees to -60 degrees and 60 degrees to 120 degrees, otherwise the results cannot be trusted due to the above-mentioned non-linearity effects of the AD 8302.

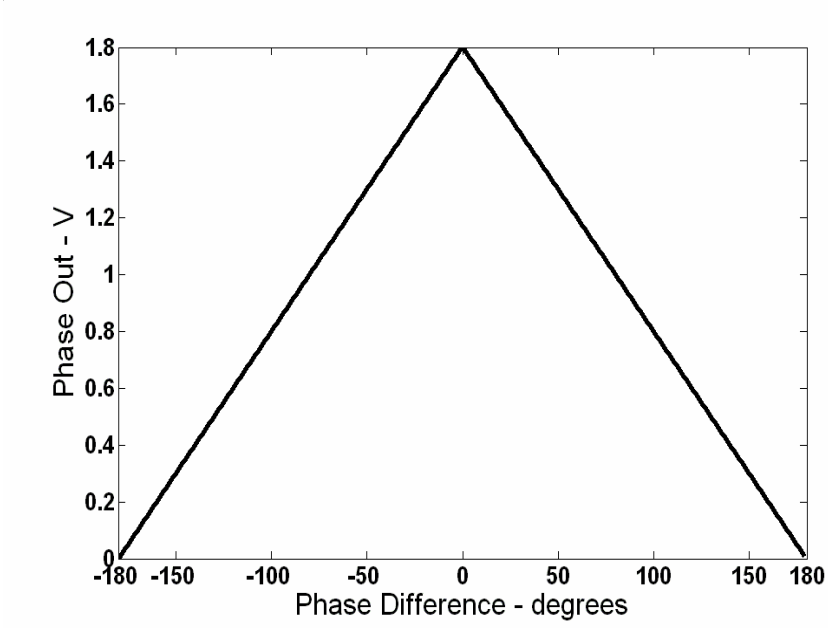


a)

Figure 4. AD8302 Phase Performance a) Ideal Performance b) Real Performance

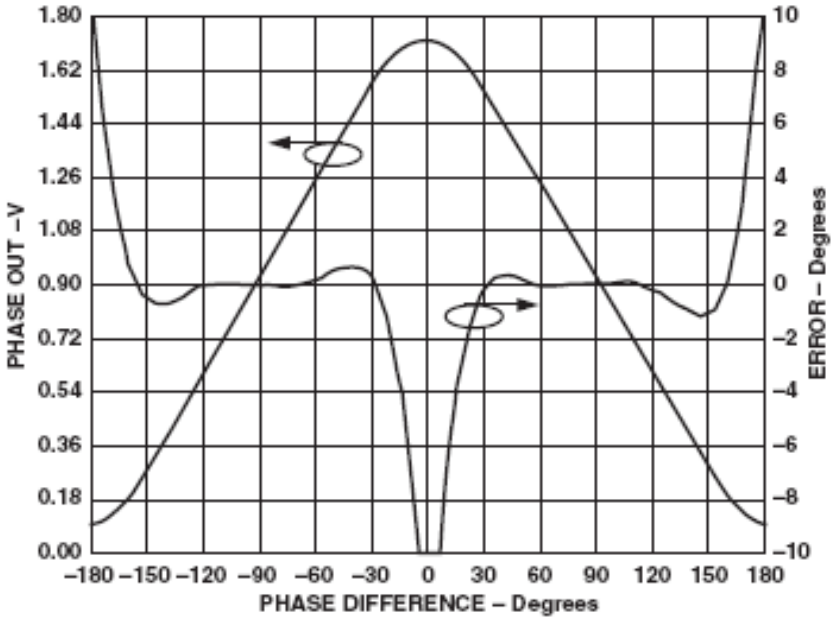


b)

Figure 4 Continued.

In a similar manner, the magnitude ratio measured between the two channels of the AD 8302 has a small error that occurs at the edge regions of detection. An ideal $V_{gain}$ output would consist of a simple ramp function that starts at -30 dB (0 Volts) and ends at 30 dB (1.8 Volts). An example of this waveform can be found in Figure 5a. Again, the AD 8302 has error that develops around the edges of the magnitude detection range (-30 dB and 30 dB). A typical plot of the magnitude output voltage ($V_{gain}$) can be found in Figure 5b, taken from the AD 8302 data sheet. Of course, the majority of the output magnitude data range is linear and accurate.

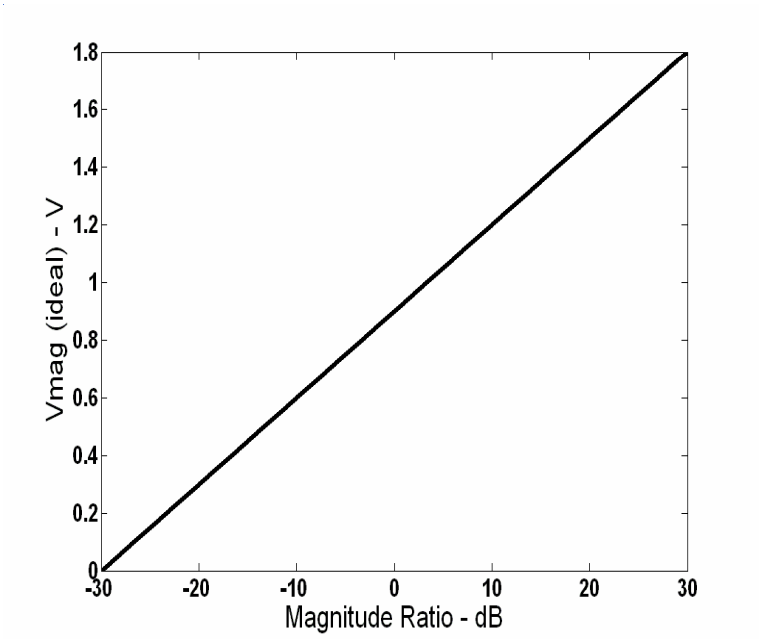


a)

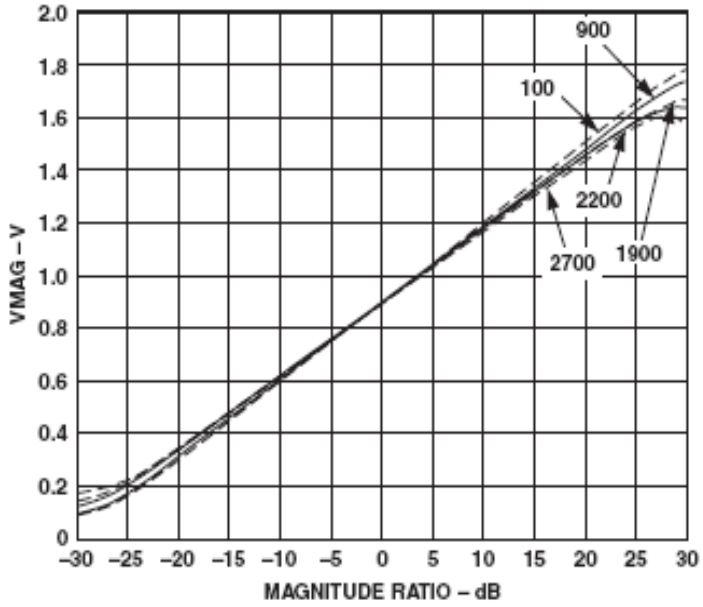


b)

Figure 5. AD 8302 Gain Performance a) Ideal Performance b) Real Performance

A performance curve of the measurement setup was taken by sweeping the phase shifter from -180 degrees to 180 degrees with a modulation frequency of 2 GHz. The results of this test can be seen in Figure 6. The performance curve of the measurement setup resembles the curve taken from the AD 8302 data sheet. Typically, the AD 8302 performs better with lower frequencies. However, more electrical noise was noted at lower frequencies using the HP RF source. Since the AD 8302 data sheet has established the performance of the AD 8302 at lower frequencies, the HP RF source is the suspected cause of the increase in electrical noise at lower modulation frequencies.

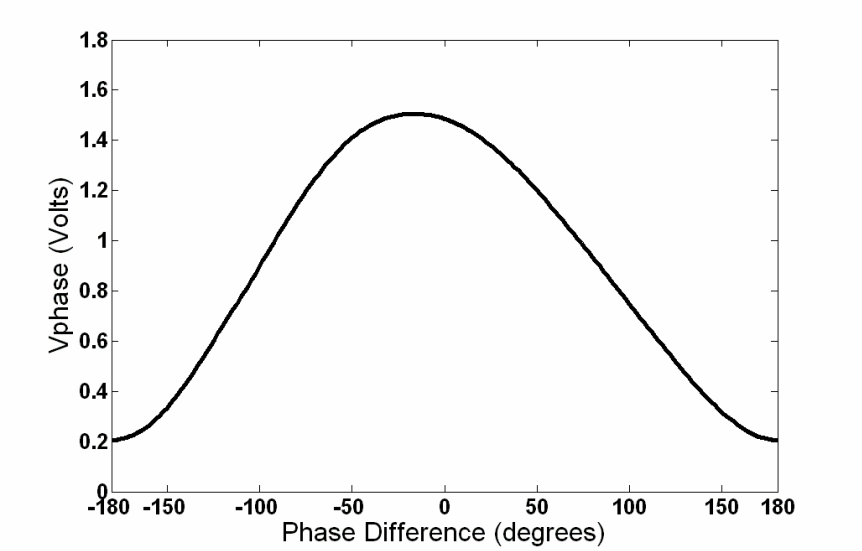


Figure 6. Vphase Performance Curve from Measurement Setup

Another source of error associated with the phase measurement of the AD 8302 develops from drift on the Vphase output voltage. A measurement test was run where

all of the components in the setup were kept constant and the $V_{phase}$ output was monitored for a duration of 120 minutes. The results, given in degrees with respect to minutes, can be seen in Figure 7. Over the course of 120 minutes, about 60 degrees of shift was observed. A linear regression analysis shows the average drift in Table 2. If lengthy measurements are taken with the AD 8302, then there will be an offset that develops in the phase measurement which will lead to phase inaccuracies. Since all of the components in the measurement setup were kept constant in this test, the likely cause of the phase measurement drift is temperature or drifts found in the RF source. Both the simple method and phase-error compensation method are so fast that measurements are typically taken in a second or less. Therefore, this source of error is not a significant contributor.

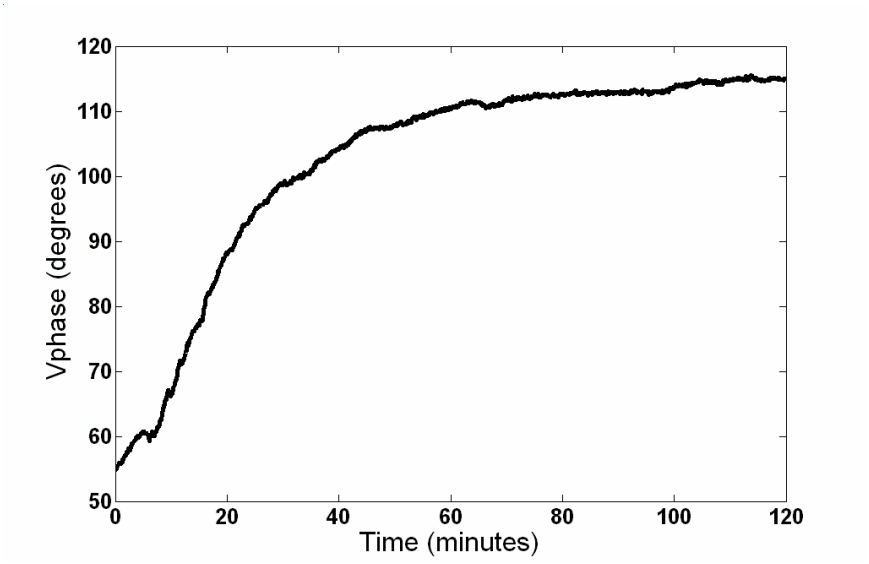


Figure 7. Vphase Drift Test

Table 2. Vphase Drift Linear Regression Results

| Time | Average Drift (degree/sec) |
|---|---|
| **0-30 minutes** | **0.0277** |
| **30-60 minutes** | **0.0066** |
| **60-120 minutes** | **0.0012** |

*Modified Test Setup for Phase-Error Compensation*

As seen previously, the AD 8302 has non-linearities that lead to phase measurement errors. Of course, the regions from –120 degrees to -60 degrees and 60 degrees to 120 degrees do not suffer from this source of error. However, the measurement setup would have to be tweaked with the phase shifter every time a phase measurement is performed in order to assure accuracy. Also, some devices under test at higher modulation frequencies could easily cause the phase measurement data to extend outside of the linear phase regions (if over 60 degrees) and accumulate error.

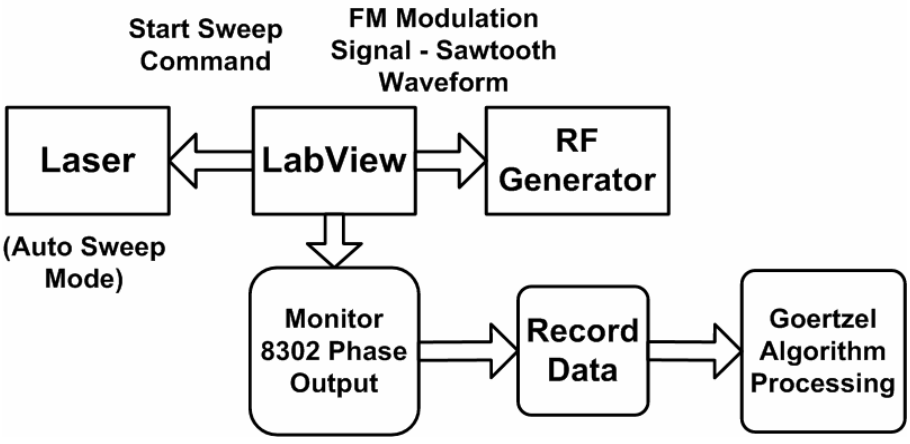


Figure 8. Measurement Setup Phase-Error Compensation Method

For these reasons, an alternate method was developed with the measurement setup to improve the performance of the phase measurement. The new method consists of frequency modulating (FM) the RF frequency such that the phase measured by the AD 8302 is swept from -180 degrees to 180 degrees for each wavelength that is desired to be measured. Once this cycle of sinusoid-like data is captured, the wavelength can be changed, the process repeated, and two cycles of sinusoid-like data for two different wavelengths are obtained. Now, the Goertzel algorithm is implemented to calculate the phase difference between the two sets of data mentioned previously. The Goertzel algorithm was chosen because it has the ability to calculate the amplitude and phase information of just the fundamental frequency, in which we are only interested in. In so doing, the phase shift between the two wavelengths encountered in the device under test can be measured. Of course, this process is repeated over an entire wavelength range, where one wavelength is selected as the reference. A block diagram of this process can be seen in Figure 8. With this method, there are no longer non-linear regions in the phase measurement since the method averages the phase over the entire measurement range of -180 degrees to 180 degrees.

A test that demonstrates the idea behind this method includes a set wavelength on the laser source and a setting of 0 degrees on the phase shifter. Next, the modulation frequency is frequency modulated with a simple ramp function from a computer. In this test, the initial modulation frequency is 2 GHz and is linearly swept to approximately 2.02 GHz. This sweep of the modulation frequency sweeps the phase measurement output of the AD 8302 over the entire 360 degree range. Following this,

the phase shifter is set to 90 degrees and the modulation frequency is again swept from 2 GHz to 2.02 GHz in order to sweep the phase measurement output across 360 degrees. A plot of the two resulting data curves as well as the FM ramp function can be seen in Figure 9.

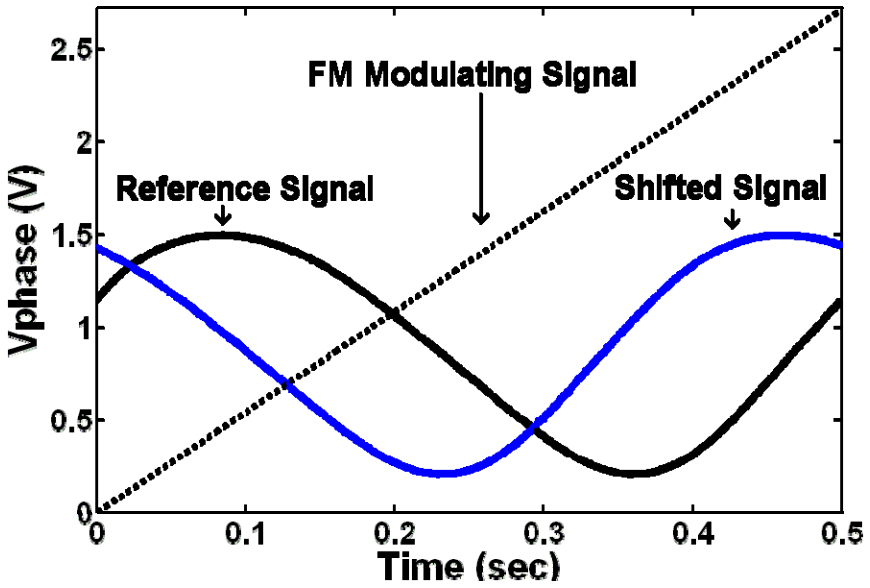


Figure 9. Phase-Error Compensation Example of Phase Detection

The Goertzel algorithm is then used to retrieve the 90 degree phase shift from these two data curves. A look at the math behind this method offers more insight to its function. As stated previously, the modulated light signal amplitude is directly proportional to $\cos(2\pi f_m t - \varphi)$ where $f_m$ is the modulation frequency and $\varphi$ is the wavelength-dependent phase shift caused by the device under test. Obviously, dispersion in the device under test normally varies $\varphi$. However, with this method, since

the modulation frequency is swept for each wavelength step, φ remains constant. However, due to the math, it is as if φ is swept from -180 degrees to 180 degrees when the modulation frequency is swept. The advantage of this method is of course is that the non- linearities do not affect the phase measurement and that no calibration would be needed so that an effective measurement range of -180 degrees to 180 degrees could be implemented with the AD 8302.

It is important to determine that the phase-error compensation method is successful in overcoming the non-linearities of the phase detection of the AD 8302. A test was completed using an Acetylene gas cell as the device under test, where the phase-error compensation method was calibrated to be in both linear and non-linear regions of the phase measurement range so that a comparison could be made. Using the HP RF source with a modulation frequency of 2 GHz, seven tests were run with a 60 degree phase shift for each consecutive test. The average standard deviation between all seven tests is 0.24 ps. The results, labeled according to the starting location with respect to Figure 4b, can be seen in Figure 10 and it can be concluded that the phase-error compensation method overcomes the non-linearities of the AD 8302 phase measurement. The magnitude plot of the same wavelength range of the gas cell can be found in Figure 11.

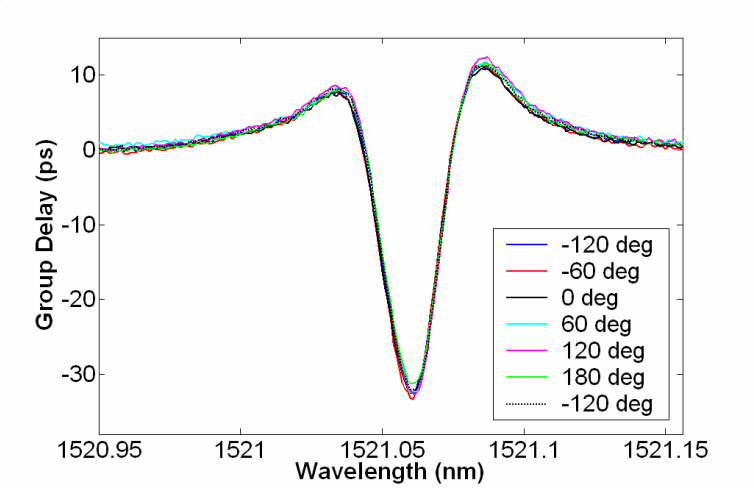


Figure 10. Phase-Error Compensation Consistency Test

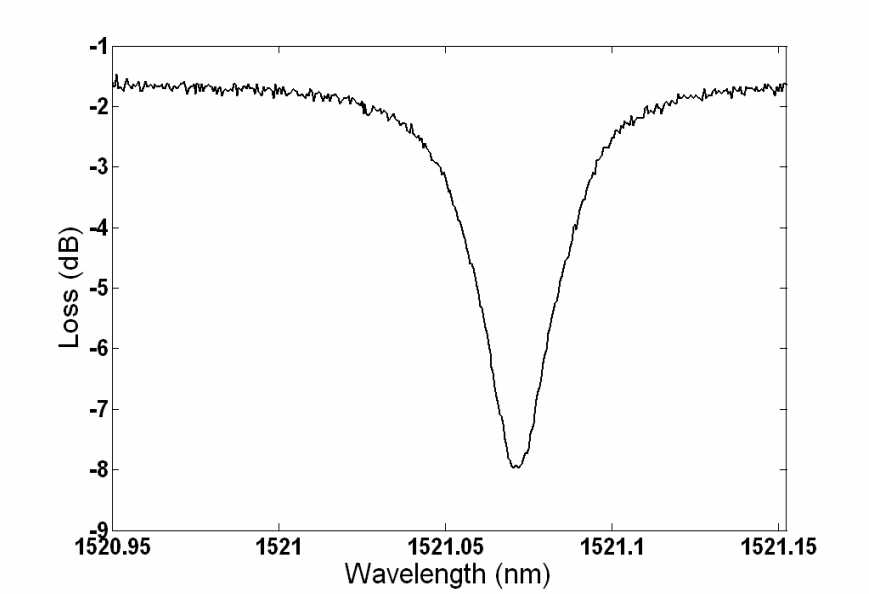


Figure 11. Phase-Error Compensation Magnitude Plot

The phase-error compensation method is implemented by controlling the frequency modulation of the RF source with the data acquisition board that also captures the AD 8302 output voltages. A software flow diagram of the phase-error

compensation method can be found in Appendix B. In order to maximize measurement speed, limited by the sweeping speed of the laser source, a continuous sawtooth waveform is sent to the RF generator in order to modulate the RF frequency continuously, generating continuous data sets as the laser sweeps. The computer then post-processes the entire data file in Matlab, pulling out the sets of data for each wavelength, comparing them to the reference wavelength with the Goertzel algorithm to obtain the wavelength-dependent phase shift, and then plotting the resulting phase-shift versus wavelength. The algorithm for this process, implemented in Matlab script in LabView, can be found in Appendix C. The entire process is synchronized by an output trigger pulse sent from the Agilent laser source at the beginning of the sweep. A GPIB protocol is used to change sweep settings and to start the actual wavelength sweep on the Agilent laser source. An illustrative example of this process can be found in Figure 12.

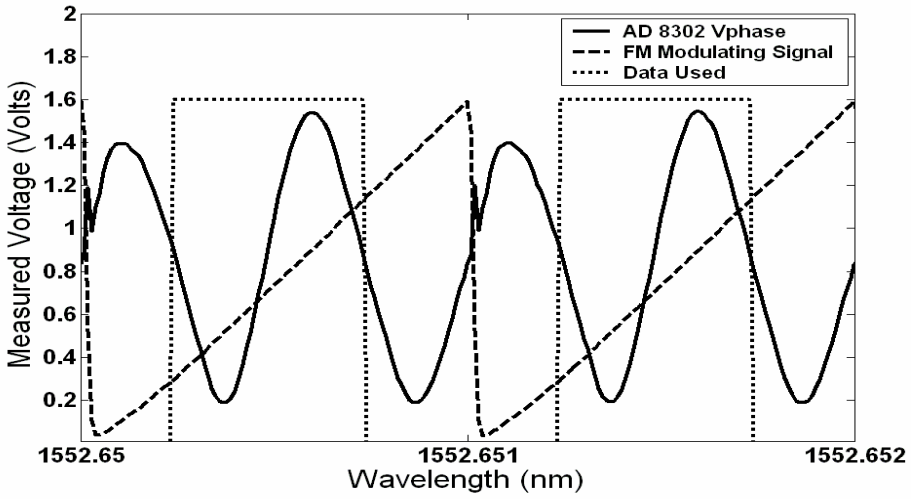


Figure 12. Data Processing of Phase-Error Compensation Method

**Performance**

Several tests were done to characterize the performance of the measurement setup. The target goal for speed was obtained in this project since the speed is only limited by the sweeping laser source, which is 40 nm/sec for the Agilent 81682A. It must be noted that calibration is required for magnitude and phase measurements with the setup. This is easily accomplished by removing the device under test and connecting the setup, followed by taking magnitude and phase measurements. This data can then be subtracted from the device under test data. The accuracy level on the magnitude and phase measurements was established by running several tests, including tests to determine the repeatability of magnitude and phase measurements, a linearity test for gain measurements, a comparison of the setup's magnitude measurements to those of a commercially available instrument (Micron Finisar) to determine absolute magnitude accuracy, an analysis on the accuracy of the Goertzel method in determining phase shifts, a comparison of the phase-error compensation method to the simple method for phase measurements, and a comparison between the setup's phase measurements to the Hilbert Transform method using measured magnitude data to determine absolute phase accuracy.

An important factor in the accuracy of the measurement setup is repeatability of the magnitude and phase measurements. Tests were run on data from the magnitude performance and phase performance, taken by the simple method and phase-error compensation method. The Micron Finisar measurement system was included in this test for comparison. For the gain measurement repeatability, ten sets of data were taken

with the simple method over a wavelength range of 1512 nm to 1542 nm using an Acetylene gas cell as the device under test. With this optical device, a max peak to peak magnitude change was observed at approximately 8 dB. Both the Wiltron and HP RF sources were used at modulation frequencies of 500 MHz, 1 GHz, 1.5 GHz, and 2 GHz. For each method, the standard deviation was then taken between the ten data sets for each single wavelength step. Next, a standard deviation was taken of these results in order to obtain an average deviation across the entire wavelength range for each method. The results can be seen in Table 3.

Table 3. Gain Measurement Repeatability Results

| Method | Standard Deviation (10 sets) | Peak Std Deviation (10 sets) |
|---|---|---|
| Wiltron (2GHz) | 0.0144 dB | 0.1872 dB |
| HP Simple (0.5GHz) | 0.0366 dB | 0.2845 dB |
| HP Simple (1GHz) | 0.0184 dB | 0.1801 dB |
| HP Simple (1.5GHz) | 0.0145 dB | 0.1438 dB |
| HP Simple (2GHz) | 0.0171 dB | 0.2136 dB |
| Finisar | 0.0084 dB | 0.1284 dB |

In order to determine the phase measurement repeatability, ten sets of data were taken with the simple method and the phase-error compensation (PEC) method over a smaller wavelength range than before, from 1520 nm to 1522 nm using an Acetylene gas cell as the device under test. Both the Wiltron and HP RF sources were used at modulation frequencies of 500 MHz, 1 GHz, 1.5 GHz, and 2 GHz. For each method, the standard deviation was then taken between the ten data sets for each single wavelength step. Next, a standard deviation was taken of these results in order to

obtain an average deviation across the entire wavelength range for each method. The results can be seen in Table 4.

Table 4. Phase Measurement Repeatability Results

| Method | Standard Deviation (10 sets) | Peak Std Deviation (10 sets) |
|---|---|---|
| Wiltron Simple (2GHz) | 0.0791 ps | 1.0506 ps |
| Wiltron Goertzel (2GHz) | 0.1210 ps | 0.8126 ps |
| HP Goertzel (0.5GHz) | 0.4337 ps | 5.6489 ps |
| HP Goertzel (1GHz) | 0.3967 ps | 2.8286 ps |
| HP Goertzel (1.5GHz) | 0.1689 ps | 1.4432 ps |
| HP Goertzel (2GHz) | 0.0819 ps | 0.8535 ps |
| HP Simple (0.5GHz) | 0.6472 ps | 5.1856 ps |
| HP Simple (1GHz) | 0.3397 ps | 2.6830 ps |
| HP Simple (1.5GHz) | 0.1656 ps | 1.3189 ps |
| HP Simple (2GHz) | 0.2359 ps | 2.2913 ps |

The gain linearity of the measurement setup was established by testing the setup with modulation frequencies of 500 MHz, 1 GHz, 1.5 GHz, and 2 GHz, a constant wavelength of 1542 nm, and the Acetylene gas cell as the device under test. The laser output was decreased from 5.5 dBm to 0 dBm with 0.1 dBm increments and the $V_{gain}$ output of the AD 8302 was monitored. The results of the test can be found in Figure 13. As seen in Figure 13, the ideal linearity of the AD 8302 is plotted along with the different modulation frequency results. The results conclude that the gain measurement is very linear with only a 1% or less deviation of the slopes of the different modulation frequencies when compared to the ideal 30 mV/dB sensitivity for this laser output power range. For laser output optical power below 0 dBm, the expected deviation from the ideal caused by the performance of the AD 8302 (seen in Figure 5b) is observed.

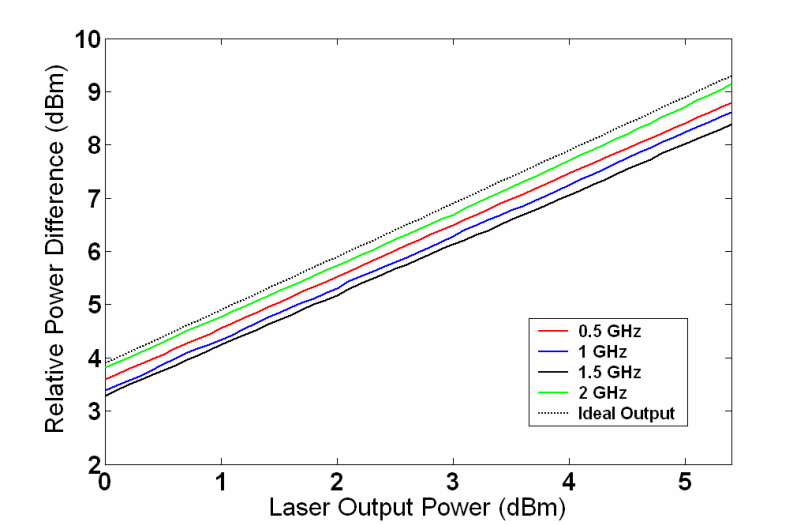


Figure 13. Gain Measurement Linearity Test

In order to classify the accuracy of magnitude measurement in the setup, the Micron Finisar, a commercially available instrument, was selected for a comparison analysis. An Acetylene gas cell was chosen as the device under test. Measurements with the setup at modulation frequencies of 0.5 GHz, 1 GHz, 1.5 GHz, and 2 GHz using the HP RF source were compared to measurement taken with the Micron Finisar and can be seen in Figure 14. The data plot features the transmission responses as loss (in dB) versus wavelength. Next, a root mean square error was taken between each of the different modulation frequencies of the measurement setup and data taken from the Micron Finisar. The results can be found in Table 5. As shown in Table 5, the error between the measurement setup and the Micron Finisar is small. The Micron Finisar uses a fiber ring laser and a gas cell as a reference. The linewidth of the Micron Finisar laser is 500 MHz compared to the 100 kHz linewidth of the Agilent laser source. The root mean square error is excellent, especially when considering uncertainties due to

connecting and disconnecting fiber connections lead to errors of the same order of magnitude.

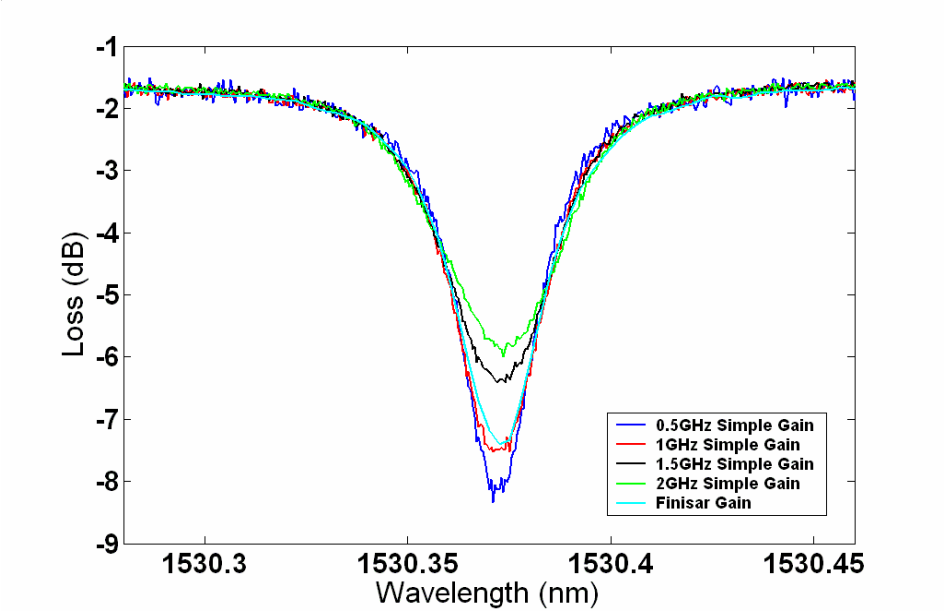


Figure 14. Gain Measurement Absolute Accuracy Plot

Table 5. Gain Measurement Absolute Accuracy Results

| Method | Root Mean Square Error |
|---|---|
| **HP Simple (0.5 GHz)** | **0.1457 dB** |
| **HP Simple (1 GHz)** | **0.1078 dB** |
| **HP Simple (1.5 GHz)** | **0.1198 dB** |
| **HP Simple (2 GHz)** | **0.1505 dB** |

It was important to establish the accuracy of the Goertzel method in its ability to detect phase shifts from data taken at different wavelengths. The Goertzel algorithm

computes the discrete Fourier transform of a desired set of data. The equations for the Goertzel algorithm are

$$v_k[n] \equiv x_e[n] + 2\cos(\frac{2\pi k}{N})v_k[n-1] - v_k[n-2]$$

$$x_e[n] = \begin{cases} x(n), 0 \le n \le N-1 \\ 0, n < 0, n \ge N \end{cases}$$

$$y_k[N] \equiv v_k[N] - W_N^k v_k[N-1]$$

In the above equations, n is the index of the test signal, N is the number of samples of the discrete Fourier transform, k is a computed index term, x(n) is the test signal, W is a Fourier coefficient, and $v_k$ is an intermediate array. Once the Goertzel algorithm calculates the discrete fourier transform for a reference set and test set of data, the maxima are found for both. Next, the phase angle is taken from the result of the maximum frequency element of the reference set divided by the maximum frequency element of the test set. Since both data sets should be the same frequency, this answer reveals the phase shift between reference and test data.

The Goertzel algorithm is sensitive to sets of data that are not approximately one cycle in nature. A simple simulation that illustrates this fact includes phase shifting ideal sine wave data taken at varying fractions of a cycle and then processing this data with the Goertzel algorithm. Basically, for the different percentages of data cycles (100%, 99%, 98%, 101%, and 102%) a reference ideal sine wave with a 0 degree phase shift was compared to an ideal sine wave with a phase shift sweep from 1 to 360 degrees (1 degree steps) using the Goertzel algorithm. Next, a root mean square error was taken between the actual phase shift and the calculated shift from the Goertzel

algorithm. The accuracy results can be found in the Table 6. As seen in Table 6, the Goertzel algorithm is very sensitive to having a full cycle of data. Therefore, the ability to ensure that data sets taken with the phase-error compensation method are within 1% of a complete cycle was integrated into the Labview program by allowing the user to adjust the voltage range of the output FM modulation signal. This is accomplished by subtracting the last $V_{phase}$ voltage sample from the first $V_{phase}$ voltage sample and showing the user the result. Since the target $V_{phase}$ signal is a one cycle sinusoidal function, the user has the option to increase the output FM modulation signal voltage range if the error mentioned previously is less than one cycle of sinusoidal data and that more FM modulation is needed to obtain a full cycle. The process works the same if the error mentioned previously is more than one cycle and less FM modulation is necessary. The user can quickly isolate the correct FM modulation signal voltage range by making the subtraction error approximately zero.

Table 6. Goertzel Algorithm Ideal Test Results

| Method | Root Mean Square Error |
|---|---|
| **Ideal Sine Wave (perfect cycle)** | **0 degrees** |
| **Ideal Sine Wave (1% under cycle)** | **0.2069 degrees** |
| **Ideal Sine Wave (2% under cycle)** | **0.4234 degrees** |
| **Ideal Sine Wave (1% over cycle)** | **0.2017 degrees** |
| **Ideal Sine Wave (2% over cycle)** | **0.4030 degrees** |

Next, phase measurements were made with the setup using the manual phase shifter to induce planned phase shifts in order to see how accurately the Goertzel method could recover these phase shifts. Basically, initial testing included a phase shifter setting of 0 degrees and 90 degrees, where starting frequencies of 500 MHz, 1 GHz, 1.5 GHz, and 2 GHz were tested at each of the phase settings using the HP RF source. The phase shifter setting of 90 degrees translates to a frequency dependent phase shift, where the real shift is equal to the setting of the phase shifter multiplied by the modulation frequency in GHz. As stated previously, the Goertzel method includes frequency modulating the RF drive signal. For example, in this test, the RF source was linearly swept from 2 GHz to 2.015 GHz. Depending on the relative delay between the optical and reference paths, different FM sweeps are required for one period of the RF phase response ($V_{phase}$). By noting this frequency shift, the relative delay can be calculated. A table of the results can be found in Table 7. The results conclude the Goertzel method has the ability to detect a phase shift within approximately 1 degree of error. It must be noted that there is a definite uncertainty in the manual setting of the RF phase shifter. Therefore, the results in Table 7 include the phase shifter uncertainty as well.

Table 7. Goertzel Algorithm Real Results (RF Phase Shifter)

| Method | Error Standard Dev. |
|---|---|
| **HP Goertzel (0.5 GHz)** | **1.0944 degrees** |
| **HP Goertzel (1 GHz)** | **0.8682 degrees** |
| **HP Goertzel (1.5 GHz)** | **0.4808 degrees** |
| **HP Goertzel (2 GHz)** | **0.7851 degrees** |

Since the phase-error compensation (PEC) method overcomes the non-linearities of the AD 8302, it is important that the phase measurement accuracy level be equal to the simple method when operating in the linear phase regions. An Acetylene gas cell was chosen as the device under test and the phase-error compensaition method was used to collect the phase measurement from 1520 nm to 1522 nm. Next, the simple method was used over the same wavelength region where the phase shifter was calibrated so that the simple method could operate practically error-free by placing it in the linear region of -120 degrees to -60 degrees. The data from the two methods were then compared. This test was run at modulation frequencies of 500 MHz, 1 GHz, 1.5 GHz, and 2 GHz using the HP RF source. The results of the test can be found in Table 8. An analysis of the error between the two measurements was done by simply taking the root mean square error between the two methods for each modulation frequency. As seen in Table 8, the error between frequencies of 1 GHz, 1.5 GHz, and 2 GHz is small. The larger error seen with 500 MHz is due to electrical noise that the HP RF source acquires at lower frequencies.

Table 8. Phase Simple Versus Phase-Error Compensation Methods

| Method | Root Mean Square Error |
|---|---|
| **HP Simple vs PEC (0.5 GHz)** | **7.0622 ps** |
| **HP Simple vs PEC (1 GHz)** | **2.7162 ps** |
| **HP Simple vs PEC (1.5 GHz)** | **1.4655 ps** |
| **HP Simple vs PEC (2 GHz)** | **1.1576 ps** |

In testing the absolute accuracy of phase measurements taken by the setup, the Hilbert Transform was used to calculate the ideal optical phase performance of an Acetylene gas cell. The Hilbert Transform can be used to calculate ideal optical phase from measured magnitude data for all minimum-phase optical devices. The easiest method for this is given by the equation

optical phase = fft {[-j sign(k)] [ifft ( log | magnitude data | ) ] },

where fft is the fast Fourier transform, ifft is the inverse fast Fourier transform, sign is the Signum function, k is an array centered at 0 which corresponds to the optical frequency, and log is the natural logarithm. Matlab code that implements this method can be found in Appendix C. Basically, since the group delay versus wavelength is measured for the device under test, a cumulative integral of the data leads to the optical phase versus wavelength. So, a comparison between the ideal optical phase (from magnitude measurement) and the measured optical phase (integration of measured group delay) was completed. The magnitude response of the Acetylene gas cell obtained by using the HP RF source at a modulation frequency of 500 MHz was

transformed (using the Hilbert Transform method) into the ideal optical phase response. Next, the group delay response of the Acetylene was measured with the phase-error compensation method at a modulation frequency of 2 GHz. The gas cell group delay response was then integrated to obtain the measured optical phase response. A plot of the results can be seen in Figure 15, while the magnitude response for this region can be found in Figure 16. The root mean square error between these two data curves is 0.1 radians.

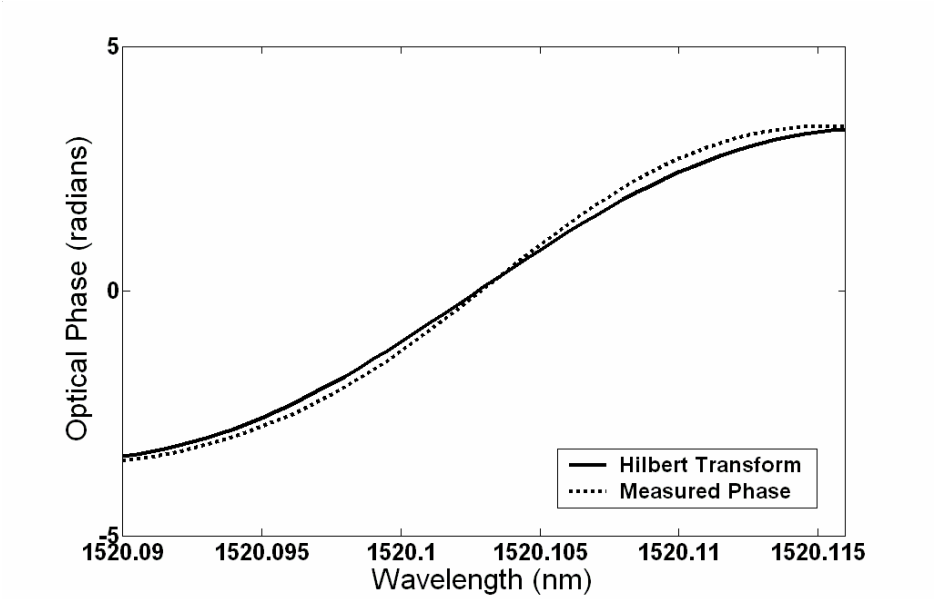


Figure 15. Optical Phase Measurement of Acetylene Gas Cell

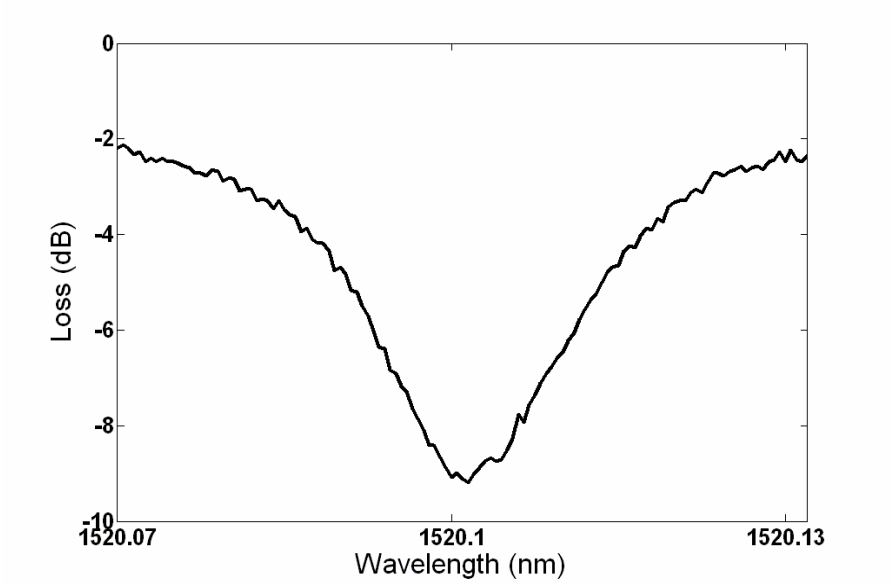


Figure 16. Optical Phase Measurement Magnitude Reference

**Device Testing**

After the performance of the measurement system was characterized with the tests discussed in the previous section, the setup was used to measure the gain and phase responses of an Acetylene gas cell, a Bragg grating, and a chirped Bragg grating. The simple method was used to obtain the magnitude responses and the phase-error compensation method was used to measure the phase responses. The tests for the three devices included parameters as follows: a modulation frequency of 2 GHz, output RF power of 16 dB, output Laser power of 5.5 dB, magnitude wavelength resolution of 0.5 pm, and a phase wavelength resolution of 1 pm. The HP RF generator and Agilent sweeping laser were used for these tests. Detailed information about the devices tested in this section can be found in Appendix A.

### *Acetylene Gas Cell*

An Acetylene gas cell was measured as the device under test. The magnitude results, shown in Figures 17 and 18, cover a 30 nm wavelength sweep using the Agilent laser source.

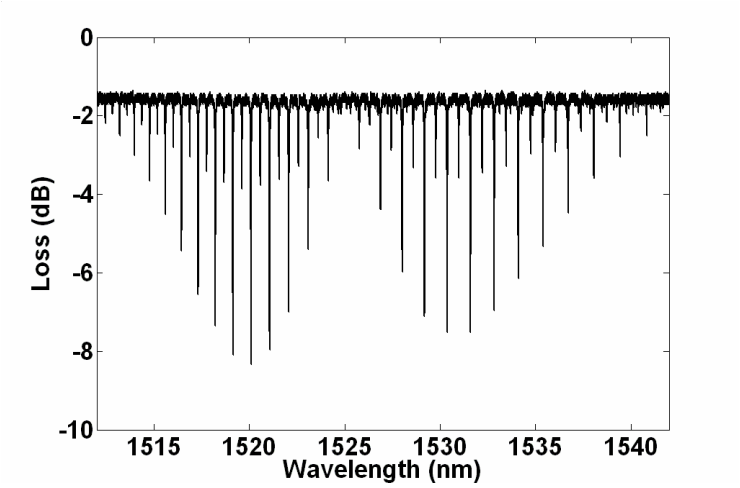


Figure 17. Acetylene Gas Cell Magnitude Response

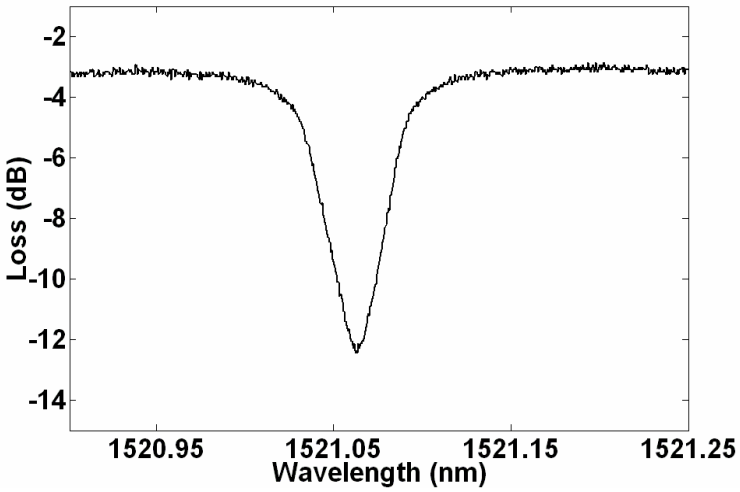


Figure 18. Acetylene Gas Cell Magnitude Response of Absorption Line

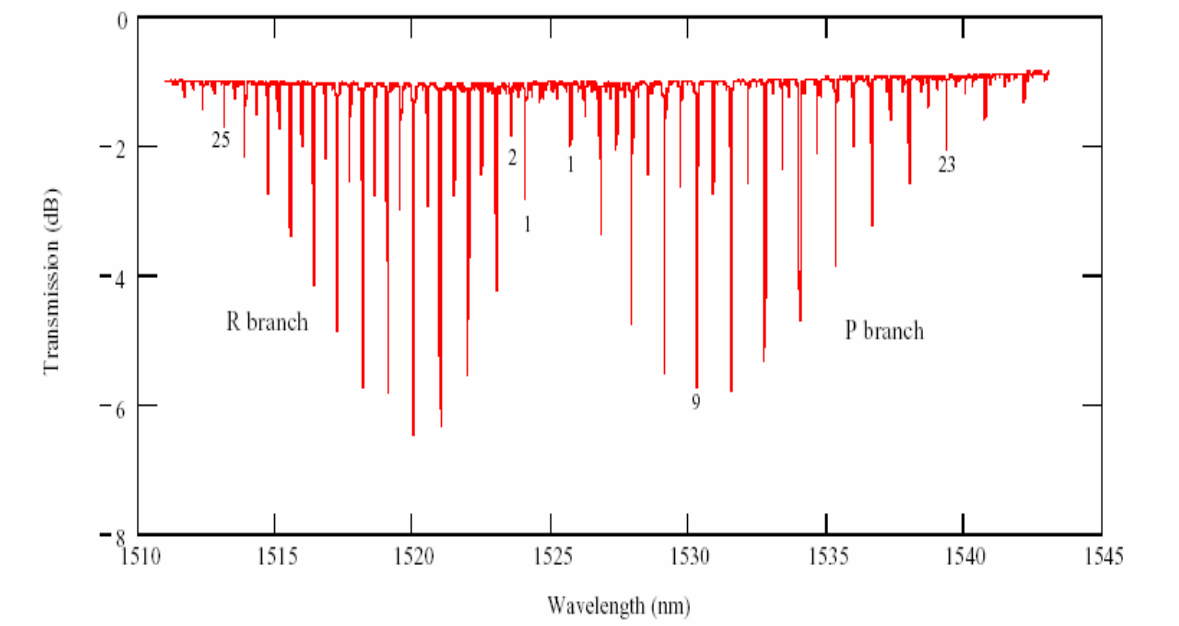


Figure 19. Acetylene Gas Cell Data Sheet Specification

When comparing the magnitude responses seen in Figures 17 and 18 to the specification plot from the data sheet seen in Figure 19, the absorption lines match closely. Table 9 depicts the deviation of the absorption lines with respect to the specifications. It can be concluded that the Agilent laser source has a wavelength offset of approximately 30 pm. However, since the offset is consistent, it is conclusive that the Agilent laser source has a very linear wavelength sweep. The measured group delay of one of the spectra can be found in Figure 20.

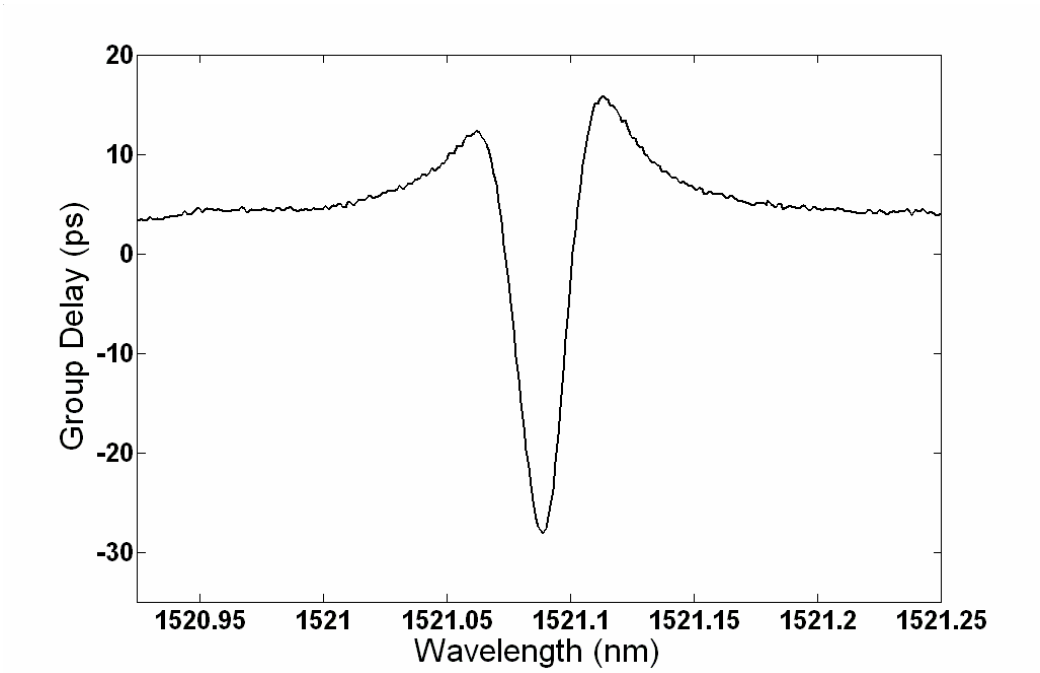


Figure 20. Acetylene Gas Cell Phase Response of Absorption Line

Table 9. Acetylene Gas Cell Specification Comparison

| | Spec | Bragg Grating - DUT Gas Cell (Reference) | Diff. | Gas Cell - DUT | Diff. |
|---|---|---|---|---|---|
| **9** | 1520.0864 | 1520.1150 | 0.0286 | 1520.1190 | 0.0326 |
| **8** | 1520.5704 | 1520.6000 | 0.0296 | 1520.6050 | 0.0346 |
| **7** | 1521.0608 | 1521.0880 | 0.0272 | 1521.0940 | 0.0332 |
| **6** | 1521.5574 | 1521.5835 | 0.0261 | 1521.5900 | 0.0326 |

***Bragg Grating***

Next, a fiber Bragg grating was measured in transmission. The magnitude response over a wavelength range of 40 nm can be found in Figure 21.

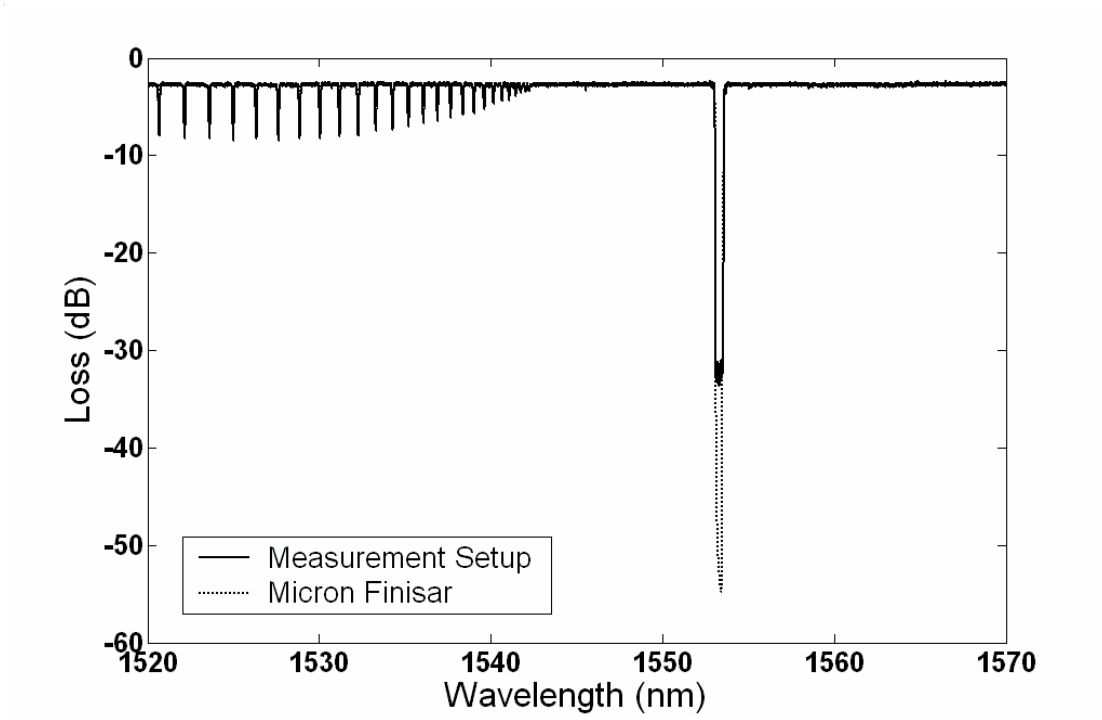


Figure 21. Bragg Grating Magnitude Response

The stopband of the bragg grating is approximately 1553 nm to 1553.6 nm and can be found in Figure 22. The dynamic range for the magnitude measurement is 30 dB, limited by the high speed detector in the setup, since a possible 60 dB dynamic range of RF power is possible with the AD 8302. The group delay around the stopband region can be seen in Figure 23. Within the stopband region, approximately 25 dB down, the group delay measurement is not accurate and practically not a concern.

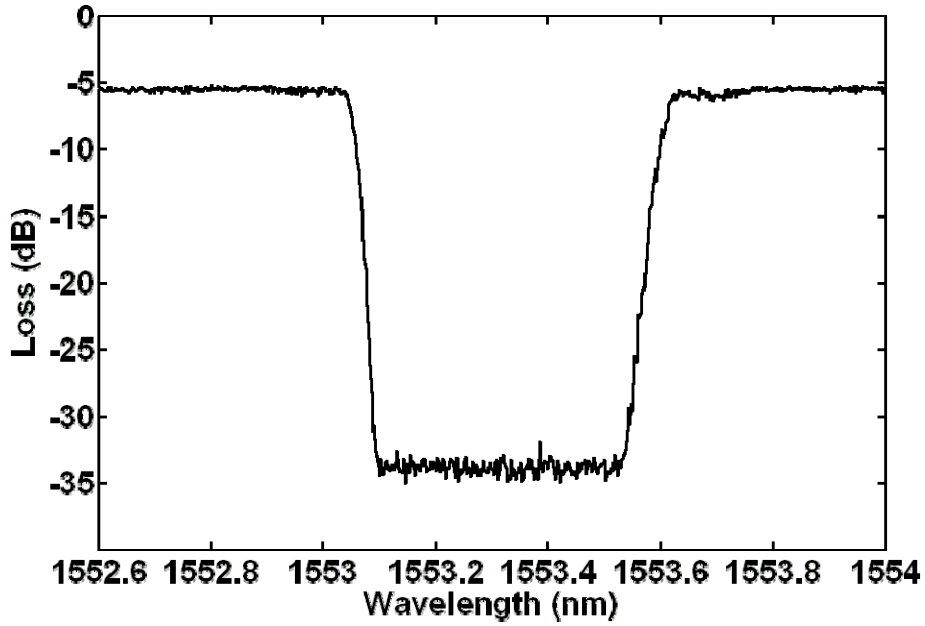


Figure 22. Bragg Grating Magnitude Response of Stopband

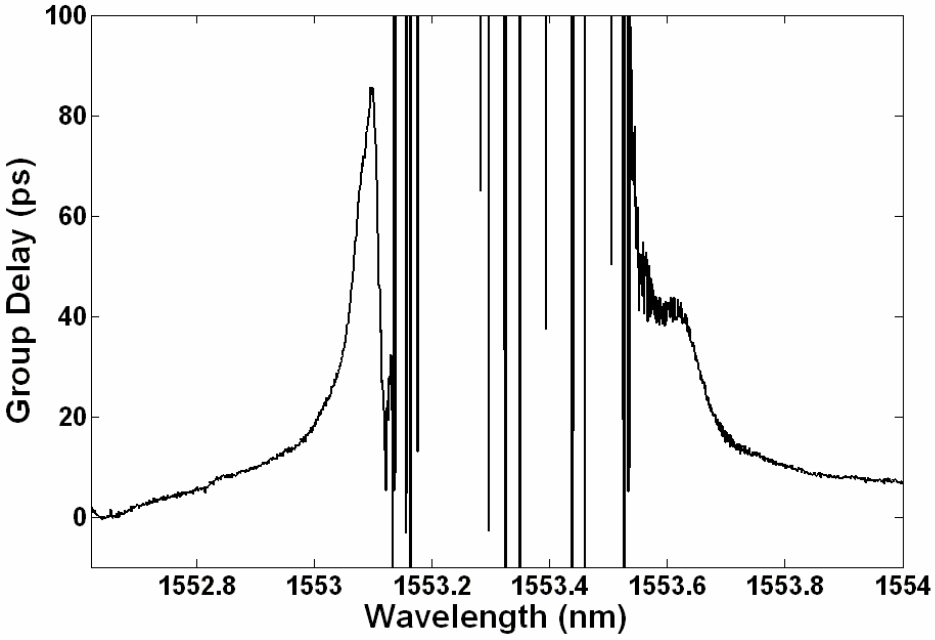


Figure 23. Bragg Grating Phase Response of Stopband

***Chirped Bragg Grating***

The third device tested with the measurement setup included a chirped Bragg grating. The magnitude response of the chirped Bragg grating was over a wavelength range of 1534 nm to 1542 nm and can be found in Figure 24. The group delay of the passband region is found in Figure 25. After taking a $10^{th}$ degree polynomial curve fitting on the group delay data found in Figure 25, the derivative was taken to find the dispersion of the passband region. The results can be found in Figure 26.

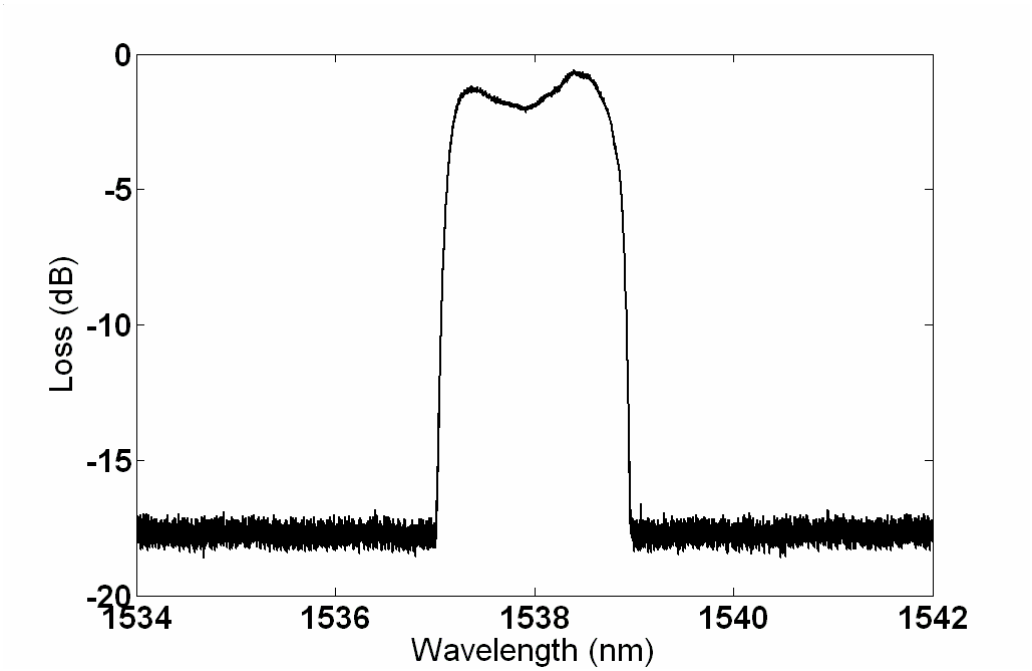


Figure 24. Chirped Bragg Grating Magnitude Response

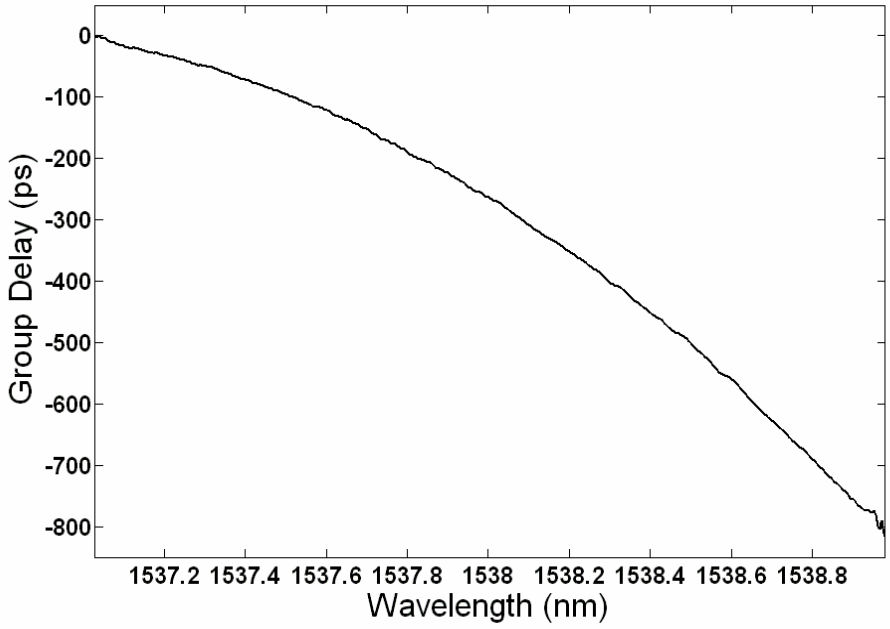


Figure 25. Chirped Bragg Grating Phase Response

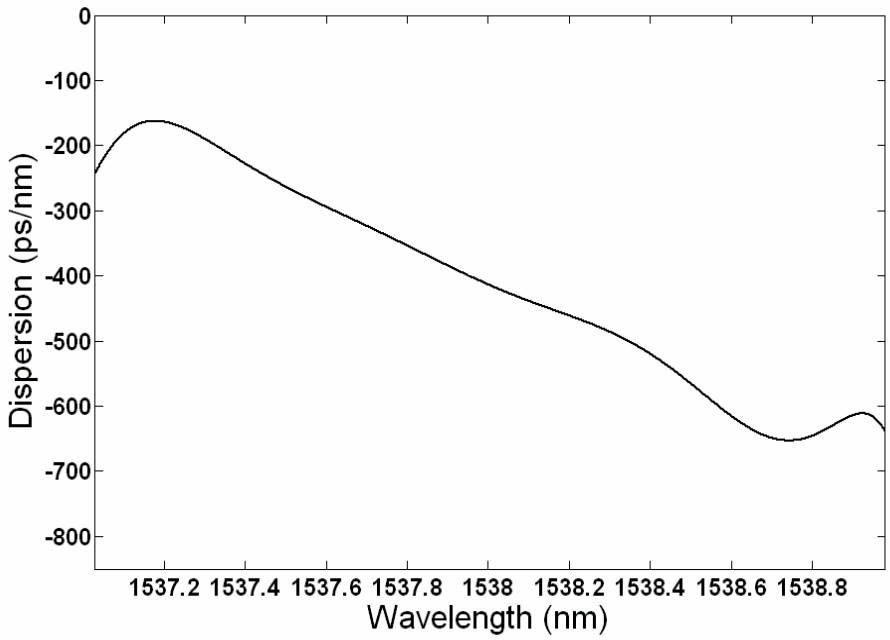


Figure 26. Chirped Bragg Grating Dispersion

# CONCLUSION

The measurement technique presented in this research thesis is fast and accurate. A novel technique which frequency modulates the RF drive signal, overcoming phase non-linearities in the measurement setup, is also presented. The measurement speed is limited by the sweeping speed of the laser source for this measurement setup at 40 nm/sec. However, the limitations of the analog output performance of the National Instruments PCI 6115 DAQ card allow sweep speeds of 80 nm/sec with a 2 pm resolution and 160 nm/sec with a 4 pm resolution. The limit is restricted by the analog output max sampling rate of 4,000,000 samples per second for the PCI 6115. Therefore, going beyond this range would cause undesired characteristics on the RF drive signal, resulting in inaccuracies with the phase-error compensation method. Since the measurement speed for a single wavelength is on the order of microseconds, the ability to sweep the modulation frequency becomes available as well as sweeping the laser wavelength. The speed of the measurement setup excels over the conventional modulation phase-shift technique which relies on a lock-in amplifier, operating at audio frequencies, for phase detection. In addition, error that accumulates from polarization dependence, temperature drift, waveguide coupling drift, and vibrations is minimized with the high speed measurement technique. The accuracy of the magnitude measurement with a modulation frequency of 1 GHz was determined to be within a 0.11 dB error when compared to the commercially available Micron Finisar measurement system. The phase accuracy was determined by taking the

integral of the measured group delay and comparing it to the ideal optical phase determined from the Hilbert Transform of the magnitude response. The measured optical phase was found to be within an error of 0.1 radians with respect to the estimated ideal optical phase. An efficient method to determine the accuracy of the dispersion measurement was not available since it would require a double derivative of the ideal optical phase in comparison to the derivative of the measured group delay. Three steps of taking the derivative would accumulate error that is not representative of the measurement setup itself and therefore the results would not be conclusive. Polarization into the device under test was neglected in this work as the devices were only minimally polarization-dependent. However, the fast speed of the measurement setup will easily enable the polarization dependence to be characterized as well. An Optical Vector Analyzer, the OVA EL offered by Luna Technologies, is based on the interferometric technique for measuring chromatic dispersion. The OVA EL claims to have an optical phase accuracy of ±0.01 radians and a group delay accuracy of ±0.1 ps. In contrast, the highest accuracy reported with the modulation phase-shift technique is ±0.46 ps [5]. The measurement setup in this research work has a lower accuracy level than both of these methods at a cost of speed. However, the repeatability of the group delay measurement performance (2GHz frequency with PEC method, Table 4) includes an average deviation of only 0.0819 ps. The economic viability of the measurement setup is also much greater since a lock-in amplifier is not required. The measurement setup can be constructed from commonly found optical laboratory instruments with the addition of the Analog Devices 8302 detector chip, whose cost is minimal at $20 per

chip currently. One outstanding feature of the measurement setup is its immunity to errors that normally develop when multiples of $2\pi$ are detected in the phase shift technique. The algorithm used in the phase-error compensation method places a noticeable shift in the measured data so that multiples of $2\pi$ are easily detected and addressed. Therefore, maximum group delay measurements of $1 / f_m$ are not a limitation with this measurement technique, and the advantage of higher modulation frequencies can be used to get better feature resolution as long as the spectral width of the device under test will accommodate it.

## REFERENCES


[1] C. K. Madsen and J. H. Zhao, *Optical Filter Design and Analysis: A Signal Processing Approach.* New York: John Wiley, 1999.

[2] T. Ozeki and A. Watanabe, "Measurements of wavelength dependence of group delay in a multimode silica fiber," *Appl. Phys. Lett.*, vol. 28, no. 7, pp. 382-383, April 1976.

[3] B. Costa, D. Mazzoni, M. Puleo, and E. Vezzoni, "Phase shift technique for the measurement of chromatic dispersion in optical fibers using LED's," *IEEE J. Quantum Electron.*, vol. QE-18, no. 10, pp. 1509-1515, Oct. 1982.

[4] *Chromatic Dispersion Measurement of Single Mode Optical Fibers by the Phase-Shift Method*, Electronic Industries Alliance/Telecommunications Industry Association, Standard Fiber Optic Test Procedure FOTP-169, Washington, DC, 1992.

[5] T. Dennis and P. A. Williams, "Achieving high absolute accuracy for group-delay measurements using the modulation phase-shift technique," *J. of Lightw. Technol.*, vol. 23, no. 11, pp. 3748-3754, Nov. 2005.

[6] L. G. Cohen, "Comparison of single mode fiber dispersion measurement techniques," *J. of Lightw. Technol.*, vol. LT-3, no. 5, pp. 958-966, Oct. 1985.

[7] D. Derickson, *Fiber Optic Test and Measurement*. Upper Saddle River, NJ: Prentice Hall, 1998.

[8] J. L. Fernando, *Two Methods Measure Chromatic Dispersion*. Test and Measurement World. Access: Feb. 5, 2006. http://www.reed-electronics.com/tmworld/article/CA197792.html

[9] K. Lefebvre, "Techniques take differing measures of chromatic dispersion," *WDM Solutions*, pp. 79-82, May 2001.

[10] *Chromatic Dispersion Measurement of Single Mode Optical Fibers by the Differential Phase-Shift Method*, Electronic Industries Alliance/Telecommunications Industry Association, Standard Fiber Optic Test Procedure FOTP-175, Washington, DC, 1992.

[11] M. J. Hackert, "Development of chromatic dispersion measurement on multimode fiber using the relative time of flight measurement technique," *IEEE Phot. Tech. Lett.*, vol. 4, no. 2, pp. 198-200, Feb. 1992.

[12] *Chromatic Dispersion Measurement of Multimode Graded-Index and Single Mode Optical Fibers by Spectral Group Delay Measurement in the Time Domain*, Electronic Industries Alliance/Telecommunications Industry Association, Standard Fiber Optic Test Procedure FOTP-168, Washington, DC, 1992.

[13] M. Tateda, N. Shibata, and S. Seikai, "Interferometric method for chromatic dispersion measurement in a single-mode optical fiber," *IEEE J. Quantum Electron.*, vol. QE-17, no. 3, pp. 404-407, Mar. 1981.

[14] M. Froggatt, E. Moore, and M. Wolfe, *Interferometric Measurement of Dispersion in Optical Components*. Luna Technologies. Access: Feb. 5, 2006. http://www.lunatechnologies.com/applications/Interferometric%20measurement%20of%20dispersion.pdf

# APPENDIX A

## Hardware Specifications:

HP 8168 Step-tunable Laser: 1450nm – 1590 nm range, 50 MHz linewidth, 9 dBm max output power

Agilent 81682A Sweeping Laser: 1480 nm – 1580 nm range, 100 kHz linewidth, 40 nm/sec max sweep speed, 6 dBm max output power

Wiltron 6637A-40 RF Sweep Generator: 2 - 18.6 GHz range, 18 dBm max output power

HP 8350A RF Sweep Generator: 0.01 - 2.4 GHz range, 16 dBm max output power

HP 83410C High Speed Detector: 300kHz – 3 GHz range

InGaAs Photo Detector, JDS Uniphase ETX 75 FITL A FJS LR ETEK: 5 GHz bandwidth, R=0.8 A/W

Transimpedance op-amp circuit: 630 kHz Signal Bandwidth

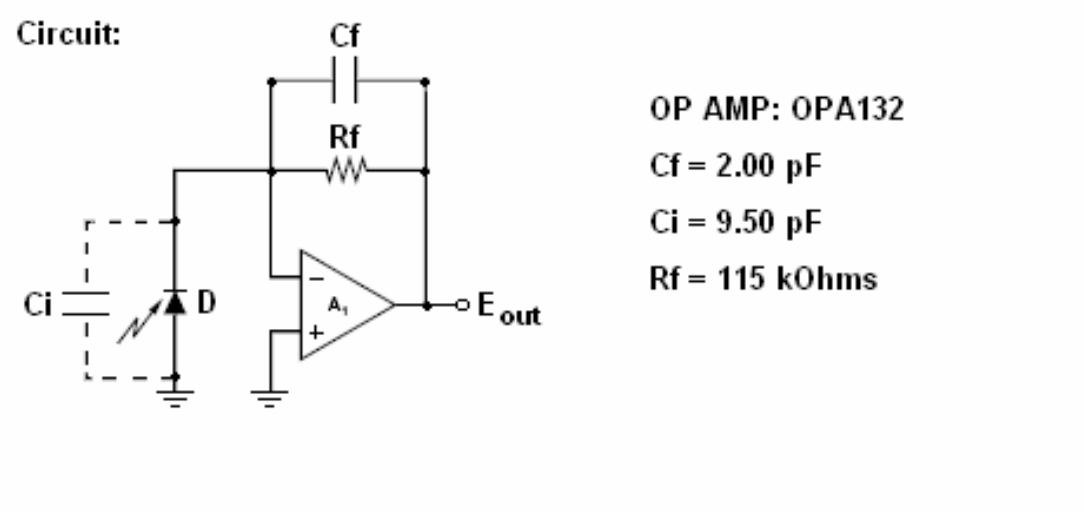


Corning OTI SD-10-A: 12.5 Gb/s bandwidth, 25 dBm max electrical, 100 mW max optical

National Instruments PCI 6115 DAQ Board: Max input sampling rate = 10E6 Samples per second, Max output sampling rate = 4E6 Samples per second, Input Signal range ±42 Volts, Output Signal range ±10 Volts

Micron Finisar: 1520 nm – 1570 nm range, 2.5 pm resolution, 500 MHz linewidth

**Device Under Test Information:**

Acetylene Gas Cell: Wavelength References, Model C2H2-12-200

Bragg Grating: JDS Uniphase, Model FBG-15-300-OT2P

Chirped Bragg Grating: Phaethon Communications, Model E00024

# APPENDIX B

## LabView Software Flow Diagram:

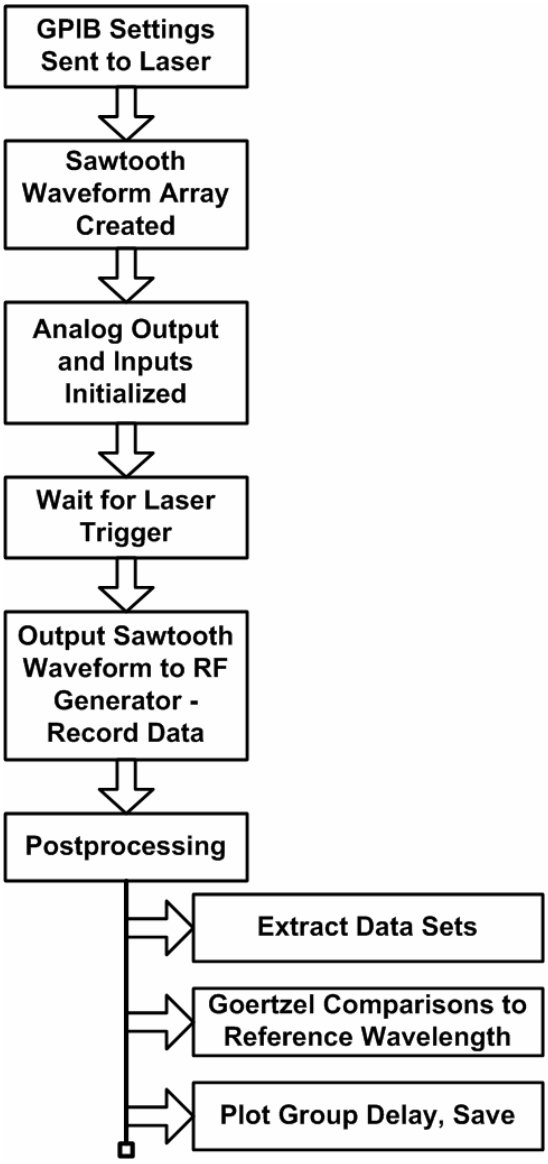

# APPENDIX C

## Matlab Code:

Hilbert Transform Code (Matlab):

```
n=length(hilbert_signal);
N=n;

k =-(n/2):(n/2-1); %k axis of DFT

w_wavelength=startwl:(stopwl-startwl)/N:stopwl-((stopwl-startwl)/N);%frequency axis
%of DFT in nm, where startwl is the start wavelength of the data, etc

hilbert_signal_nepers=a*(20/(log(10))); %original signal in dB loss, converting to
%Nepers

b=ifft(log(abs((hilbert_signal_nepers)))); %magnitude component of Fourier content,
%signal in Nepers

b2=(-j*sign(k)).*(b(1:n)); %multiply signum function in time domain
result=(fft(b2,N)); %fft this to get phase information
```

PEC Method Matlab Algorithm:

```
samplespercycle=round(samplespercycle); %where samplespercycle is the number of
%samples for each 1 cycle of desired Vphase data

xaxis=startwl:(speed*FMdt):stopwl-(speed*FMdt); %array of start wavelength to stop
%wavelength

deltaw=(stopwl-startwl)/outputcycles; %step size of the wavelength, the resolution of
%our measurement, ie 1 pm if our FM modulation process works every 1 pm
stepsize=deltaw;
%----------------------selecting what part of cycles to pull out (user selected by
%'percentage' control, typically 25% from start and 25% from end (middle data
%desired), such that 50% of the data is shaved off total)
periodstart=percentage*samplespercycle; %this is start sample number of desired data
%for each Vphase cycle
periodend=samplespercycle-(percentage*samplespercycle)-1; %this is stop sample
%number of desired data for each Vphase cycle
```

PEC Method Matlab Algorithm (continued):

```
periodstart=round(periodstart); %round to get rid of error, only want integers for
%sample numbers

periodend=round(periodend); %round to get rid of error, only want integers for sample
%numbers

samples=periodend-periodstart+1; %samples is total number of samples for 1 Vphase
%cycle
%----------------------

%====Create reference signal and pull out desired Vphase data===
trigger=0; %reset trigger each time main program is run
for n=1:outputcycles; %make boxes for all Vphase cycles, this for loop creates a box
%for each Vphase cycle and also pulls out desired cycle data of Vphase data

%----------------------Make reference signal boxes for plotting
trigger(1,(((n-1)*samplespercycle)+(periodstart)):(((n-1)*samplespercycle)
+(periodend)))=1.6; %make amplitude of box 1.6
%---------------------
%---------------------Pull out desired Vphase cycles, discarding unwanted data
goertzeldata(n,1:((1-2*percentage)*samplespercycle))=FMy(1,(((n-1)*
samplespercycle) +(periodstart)):(((n-1)*samplespercycle)+(periodend)));
%---------------------
end
%==========================================================================

ref=(refwavelength-startwl)/deltaw; %user selects the reference wavelength in which
%everything gets compared to, this is sample number of that wavelength
ref=round(ref);

%----------------------Goertzel Algorithm
FMgoertzel=0; %reset this array to clear memory
FMgoertzelx=0; %reset this array to clear memory

FMref=goertzeldata(ref,1:(samples)); %calculate goertzel dft of our reference
%wavelength
y=FMref;
ymean=mean(y); %calculate DC bias of y signal
y=y-ymean; %remove DC bias
range=1:50; %only take first 50 dft's (the power of the Goertzel algorithm!)
```

PEC Method Matlab Algorithm (continued):

```
yg = goertzel(y,range);  % Now use Goertzel to obtain the PSD for each wavelength
%step
[z,yg_correct_sample]=max(yg); %Grab the sample number which is our target
%frequency

for i=1:outputcycles %for all of our Vphase data sets

FMshifted=goertzeldata(i,1:(samples)); %calculate goertzel dft of each wavelength step
x=FMshifted;
%Subtract mean to remove DC offset
xmean=mean(x); %calculate DC bias of x signal
x=x-xmean; %remove DC bias
xg = goertzel(x,range);  % Now use Goertzel to obtain the PSD for reference signal

[z,xg_correct_sample]=max(xg); %Grab the sample number which is our target
%frequency

FMgoertzel(1,i)=angle(yg(1,yg_correct_sample)/xg(1,xg_correct_sample))*180/pi;
%Calculate %actual shifted angle between signals
FMgoertzelx(1,i)=startwl+(deltaw*i)-deltaw;
end
%-----------------------------
onecycletime=totalsamplingtime/outputcycles; %gives us the time it takes for one
%Vphase data set to be taken

figure(1)
plot(xtime,FMy,'b','linewidth',2)
title('Example of Data Taken (1st few cycles)')
xlabel('Wavelength (nm)')
ylabel('Voltage (Volts)')
hold on
plot(xtime,FMy2,'r','linewidth',2)
plot(xtime(1,1:length(trigger)),trigger,'g','linewidth',2)
hold off
axis([ (startwl+ref*stepsize) (startwl+(10+ref)*stepsize) 0 2.5])

figure(2)
plot(FMgoertzelx,FMgoertzel,'linewidth',2)
title('Device Phase Performance Curve')
xlabel('Wavelength (nm)')
ylabel('RF Phase (degrees)')
axis([startwl stopwl -180 180])
```

PEC Method Matlab Algorithm (continued):

```
figure(3)
plot(xtime,FMy,'b','linewidth',2)
title('Reference Cycle Vphase Data')
xlabel('Wavelength (nm)')
ylabel('Voltage (Volts)')
hold on
plot(xtime,FMy2,'r','linewidth',2)
plot(xtime(1,1:length(trigger)),trigger,'g','linewidth',2)
hold off
axis([(startwl+ref*stepsize-stepsize) (startwl+(ref+1)*stepsize-stepsize) 0 2.5])

s=FMy(1,ref*samplespercycle+periodstart); %calculate the voltage of the first sample
%of Vphase cycle data
e=FMy(1,ref*samplespercycle+periodend); %calculate the voltage of the last sample of
%Vphase cycle data
voltagegap=e-s; %calculate the amount of error we are away from 1 full cycle of
%Vphase data

save(filename,'FMy3','FMy2','FMy','FMsamples','FMdt','startwl','stopwl','FMgoertzelx','
FMgoertzel','stepsize','voltagegap','outputcycles','samplespercycle','percentage','xaxis',
'trigger','refwavelength','-v6')
```

Goertzel Code To determine Phase Shift:

```
%Determine phase shift between signals x and y
%Subtract mean to remove DC offset
ymean=mean(y); %calculate DC bias of y signal
xmean=mean(x); %calculate DC bias of x signal
y=y-ymean; %remove DC bias
x=x-xmean; %remove DC bias

range=1:50;
xg = goertzel(x,range);  % Now use Goertzel to obtain the PSD
yg = goertzel(y,range);  % Now use Goertzel to obtain the PSD

[z,yg_correct_sample]=max(yg); %Grab the sample number which is our target
%frequency
[z,xg_correct_sample]=max(xg); %Grab the sample number which is our target
%frequency

clear FMgoertzel
FMgoertzel(1,1)=abs(angle(yg(1,yg_correct_sample)/xg(1,xg_correct_sample))*180/pi
) %Calculate actual shifted angle between signals
```

# VITA

Name: Michael Thomas Thompson

Address: Department of Electrical and Computer Engineering
C/O Dr. Christi Madsen
Texas A&M University
214 Zachry Engineering Center
College Station, TX 77843-3128

Email Address: oiceman@gmail.com

Education: M.S., Electrical Engineering, Texas A&M University, 2006
B.S., Electrical Engineering, Louisiana Tech University, 2004